
# Modulating the Formation of Coke to Improve the Production of Light Olefins from CO2 Hydrogenation over In2O3 and SSZ-13 Catalysts

energy&fuels



pubs.acs.org/EF
Article

# Modulating the Formation of Coke to Improve the Production of Light Olefins from $CO_2$ Hydrogenation over $In_2O_3$ and SSZ-13 Catalysts

*Published as part of Energy & Fuels virtual special issue "Recent Advances in CO2 Conversion to Chemicals and Fuels".*

Wei Di, Abdenour Achour, Phuoc Hoang Ho, Sreetama Ghosh, Oleg Pajalic, Lars Josefsson, Louise Olsson, and Derek Creaser*

Cite This: https://doi.org/10.1021/acs.energyfuels.3c03172



**ABSTRACT:** Moderately acidic aluminophosphates (SAPOs) are often integrated with methanol synthesis catalysts for the hydrogenation of $CO_2$ to olefins, but they suffer from hydrothermal decomposition. Here, an alternative SSZ-13 zeolite with high hydrothermal stability is synthesized and coupled with an $In_2O_3$ catalyst in a hybrid system. Its performance regarding selectivity for olefins and coke formation was investigated for $CO_2$ hydrogenation under varying temperatures and pressures. Various reactions occur, producing mainly CO and different hydrocarbons. The results indicate that the hydrogenation of hydrocarbons are dominant at high temperatures (around 400 °C) over SSZ-13 zeolite with a high acid density and that the coke deposition rate is slow. Polymethylbenzenes are the main coke species, but the selectivity for light olefins is low among hydrocarbons at high temperatures. However, at low temperatures (around 325 °C), and especially under high pressure (40 bar), methanol disproportionation becomes significant. This results in an increased selectivity for light olefins; however, it also leads to a rapid coke deposition, which gives inactive adamantanes as the main coke species that block the pores and cause rapid deactivation. However, after coking at 325 °C and regeneration at 400 °C under the reaction atmosphere, the accumulated adamantanes can be decomposed into smaller coke species, which reopens the channel structure and generates modulated active sites within the zeolite, resulting in a higher yield of olefins without deactivation. The performances of acidic SSZ-13 zeolites, with varying ratios of Si/Al in transient experiments, further verified that a dynamic balance exists between the formation and degradation of coke within the SSZ-13 zeolite during a long-term $CO_2$ hydrogenation reaction. This balance can be achieved by optimizing the reaction conditions to match the acid density of the catalyst. Using the conditions of 20 bar and 375 °C, with a $H_2$ to $CO_2$ mole ratio of 3, the results obtained for the precoked hybrid catalysts of $In_2O_3$ and SSZ-13 (Si/Al = 25) exhibited very stable activity, with the selectivity for light olefins (based on hydrocarbons formed) of max. 70% after 100 h time-on-stream. This work provides new insights into the design of stable hybrid catalysts, especially the influence of a precoking process for SSZ-13 zeolite in the production of light olefins.

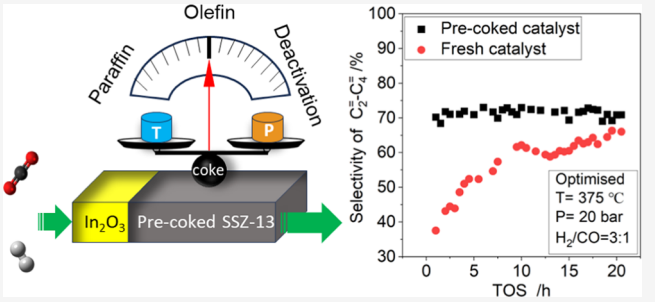




## 1. INTRODUCTION

The use of $CO_2$ rather than fossil resources as a feedstock to synthesize high-value light olefins by hydrogenation is a sustainable way of producing these carbon-based building blocks in the future.[1−5] The direct hydrogenation of $CO_2$ into olefins is, nevertheless, challenging due to the extreme inertness of the $CO_2$ molecule and the high C−C coupling barrier, as well as the occurrence of many competing reactions, such as reverse water−gas shift (RWGS) and methanation reactions, leading to the formation of $C_1$ products ($CH_4$, CO) at high temperatures.[5,6] Current methods employed for this hydrogenation include the modified Fischer−Tropsch process and the indirect methanol-mediated route. However, the Fischer−Tropsch process is limited by the Anderson−Schulz−Flory (ASF) distribution, where a maximum selectivity of 42% for $C_2$−$C_4$ olefins and approximately 58% for total $C_2$−$C_4$ hydrocarbons has been reported.[7] As a result, the methanol-mediated route is expected to be more efficient in producing

Received: August 22, 2023
Revised: October 17, 2023
Accepted: October 23, 2023

light olefins in a single reactor due to the design of the hybrid catalysts, containing methanol synthesis and zeolite catalysts.[8−10]

Zeolites with a chabazite (CHA) topology (SSZ-13, SAPO-34) are the preferred catalytic components for methanol to olefin (MTO) reactions. They offer small pores (3.8 × 3.8 Å$^2$) but larger cages (10 × 6.7 Å$^2$), favoring the formation and stabilization of the reactive carbon intermediates (polymethylbenzenes and their carbonium ions), and are mainly responsible for C−C bond formation according to the accepted hydrocarbon pool (HCP) mechanism.[11] More specifically, the confined carbon intermediate species (also known as HCP species) within the zeolite act as cocatalysts for the successive assembly of methanol and dimethyl ether (DME) into larger polymethylbenzenes by methylation, from which linear light olefins (ethylene and propene) split off by their cracking. Thus, small pore but large cage zeolites enable a high selectivity for $C_2$−$C_4$ olefins during MTO reactions.[11−14] However, HCP species are also the precursors for coke as they tend to grow into polycyclic aromatic species, such as naphthalene or phenanthrenes, which leads to deactivation by not only hindering the product diffusion but also blocking pores and cavities.[15] The double roles of HCP species, therefore, make it difficult to maintain high olefin selectivity and long life of CHA zeolites simultaneously if only MTO reactions should occur.

Compared with their use for only the MTO reactions, zeolites have exhibited a longer lifetime (defined here as the time interval between the start of feeding to a breakthrough of methanol in the effluent) during methanol-mediated $CO_2$[8−10] or CO[16,17] hydrogenation. It has been found that hydrogen can decrease the coke precursor (formaldehyde, dienes),[18] and then further suppress its polycyclization with the aid of the synergistic effects of $H_2$ and $H_2O$ at high pressure.[19] Moreover, over high-acidity zeolites, it has been demonstrated that the olefins can be further hydrogenated into paraffins during the MTO reaction with cofeeding $H_2$ at high pressure, thus hindering the oligomerization of olefins from forming the harmful coke.[20] While the hydrogen inhibits the deposition of coke, it also, quite inevitably, retards the formation of HCP species without distinction.[15] Detailed research on the effect of the acid strength on MTO, with and without cofeeding $H_2$, has been carried out over fresh SSZ-13 and SAPO-34 by Shi and co-workers.[11] They found that the acid strength of the protons played a critical role in influencing the lifetime of the catalyst and the product selectivity in MTO reactions. Compared with SAPO-34, the shorter lifetime and lower ratio of olefins to paraffins during pure MTO on SSZ-13 were attributed to its faster rates of formaldehyde formation, hydrogen transfer, and the subsequent alkylation reaction to form the inactive polycyclic aromatics on higher strength Brønsted acid sites (BAS).[11] However, a longer life span and higher alkane selectivity in $H_2$ cofeeding with MTO reactions were achieved for SSZ-13 rather than for SAPO-34, which is due to its higher hydrogenation rate constants for formaldehyde, dienes, and alkenes on the same Brønsted acid sites.[11] The most recent publications show that the mildly acidic SAPO-34 zeolites promote a higher selectivity for olefins and a good lifetime in $CO_2$ or CO hydrogenation.[8−10,16,17] Hydrothermal degradation nevertheless presents a significant challenge for SAPO-34, with its limited long-term operation and regeneration under a steam atmosphere. Zhao et al. reported that the SAPO-34 zeolite framework became partially damaged after long-term MTO reactions with high-pressure $H_2$ and $H_2O$ cofeeding.[19] In contrast, SSZ-13 zeolite deserves more attention because of its superior hydrothermal stability; however, its strong acidity leads to further hydrogenation of olefins, thereby reducing the selectivity for olefins. Most reports concerning SSZ-13 zeolites are limited to the synthesis of propane or liquefied petroleum gas (LPG) during $CO_2$ hydrogenation.[21,22] Optimizing the acidity of SSZ-13 in its application in methanol-mediated $CO_2$ hydrogenation to achieve both a higher olefin selectivity and greater stability therefore presents a real challenge.

Although the varying strength of acid sites affects the formation rate of HCP species or coke precursors, the nature and amount of coke deposited also alter acid sites and the cavity sizes of zeolites, leading to different product selectivity and lifetime during the MTO process.[12,23,24] It has been proven that the increasing content of coke is favored by the selectivity for both ethene and propene, even at high methanol conversions.[12] Liu et al.[25] reported a precoking technology for depositing the specific active HCP inside the vacant cavities of SAPO-34 by cracking 1-butene and thereby improving the formation of ethene without shortening its lifetime. Moreover, it has been found that some Brønsted acid sites were covered by coke accumulated during the precoking process.[25] The continued work of Liu et al. demonstrated further that transforming heavy coke into active HCP intermediates (active coke) can also boost the selectivity for light olefins over a spent SAPO-34 zeolite following treatment with high-temperature steam. It was shown that the reinstitution of HCP inside the cavity of zeolites was equally important as recovering acidity, both of which can promote the production of light olefins.[15] Nieskens and his team,[16] on the other hand, compared the deposition of coke with the lifetime between methanol-mediated syngas to hydrocarbon and the MTO process. Their results indicated that the hydrogen pressure, the methanol pressure, and the operating temperature played roles in determining the build-up of coke and the lifetime of SAPO-34. More specifically, a lower temperature, lower hydrogen pressure, and higher methanol partial pressure can contribute to the formation of coke that, in turn, causes catalysts to deactivate. The removal of coke is favored by a higher temperature, high hydrogen partial pressure, and low methanol partial pressure and can be used for the stable CO hydrogenation into LPG.[16] Maintaining the stability of the zeolite depends on balancing the formation of coke and its removal rate. In particular, it is necessary to stabilize the cumulative balance of HCP species in order to achieve a stable and highly selective generation of olefins. The thermodynamic limitations of $CO_2$ hydrogenation to produce methanol mean that the concentration of methanol will be relatively low at high temperatures. High temperatures seem to be more helpful in alleviating deactivation caused by coke during the MTO reaction with cofeeding hydrogen,[16] but high temperatures also promote the hydrogenation of olefins, leading to a high selectivity for paraffins instead. Optimizing suitable reaction conditions to maintain both high olefin selectivity and catalyst stability is also currently a challenge.[26]

Previously, a few investigations have been devoted to studying the performance of SSZ-13 zeolites using a hybrid catalyst system for hydrogenation of $CO_2$ to light olefins, but a low selectivity to olefins was found due to the strong acidity of SSZ-13.[11,21,22] Inspired by the fact that the reaction conditions can change the coke deposition over the zeolite, and the accumulated coke can modify the acidity of zeolite under the


https://doi.org/10.1021/acs.energyfuels.3c03172
Energy Fuels XXXX, XXX, XXX−XXX

pure MTO reaction,[12,23−25,27] here, for the first time, this approach is utilized to investigate the efficient use of SSZ-13 to produce light olefins from $CO_2$ hydrogenation. In this effort, the effects of the reaction temperature and pressure on the catalytic performance and coking performance of hybrid catalysts containing SSZ-13 were systematically investigated. Transient experiments with different reaction conditions combined with spent catalyst characterization techniques, including $N_2$-adsorption, diffuse reflectance infrared Fourier transform spectra (DRIFTS), thermogravimetric analysis (TGA), gas chromatography−mass spectrometry (GC−MS), and temperature-programmed oxidation (TPO), were performed to understand the quantities and character of coke under different conditions. A dynamic balance mechanism between the formation and degradation of coke is revealed, and a precoking method is proposed for upgrading the fresh SSZ-13 to improve the selectivity for olefins and the stability of the catalyst. Finally, the balance mechanism is verified through a long-term (100 h) stability test, and the precoking modification is also confirmed to be successful in improving the reaction performance of SSZ-13 zeolite within the $In_2O_3$/SSZ-13 hybrid catalyst.

## 2. EXPERIMENTAL METHODS

**2.1. Catalyst Preparation.** The bulk indium oxide ($In_2O_3$) was prepared according to a coprecipitation method;[28] it was used for $CO_2$ hydrogenation to methanol and was found to be stable under the varying $CO_2$, CO, and $H_2$ atmosphere conditions in previous research.[29] In brief, 7.7 g of indium(III) nitrate hydrate (Sigma-Aldrich, 99.99%) was dissolved in 117 mL of deionized water before an aqueous solution of $Na_2CO_3$ (9.1 wt %) was added dropwise to the solution. This was done under magnetic stirring at ambient temperature until a pH value of 9.2 was reached. After aging for 1 h, the precipitate obtained was filtered and washed with deionized water; it was dried thereafter in a vacuum oven overnight at 60 °C. The resulting product, a powder, was then calcined at 400 °C for 3 h to obtain the crystalline $In_2O_3$ sample. All of the $In_2O_3$ oxides used in this work were from one powder mixture that was obtained by mixing several batches prepared as above.

The SSZ-13 zeolite was synthesized from a gel solution using a hydrothermal method, with *N*,*N*,*N*-trimethyl-1-adamantylammonium hydroxide (TMAdaOH) as the sole structure-directing agent (SDA).[30] The precursor gel had a molar composition of $100SiO_2$/$XAl_2O_3$/50TMAdaOH/$4400H_2O$, where $X$ = 3.33, 2.5, and 2 represent the Si/Al molar ratios of 15, 20, and 25, respectively. First, 6.97 g of TMAdaOH aqueous solution (25 wt %, Tokyo Chemical Industry Co. Ltd.) was added to 6.35 g deionized water, followed by the designated amount of $Al(OH)_3$ (Sigma-Aldrich, >99%) under stirring in ambient conditions. Then, 2.47 g of silica sol (LUDOX AS-40, 40 wt %) was added dropwise and stirred for 2 h until a homogeneous gel solution was obtained. This gel mixture was transferred to a 160 mL Teflon-lined stainless-steel autoclave and kept at 160 °C for 6 days of crystallization under 40 rpm rotation. Centrifugation was used to collect the as-synthesized sample, which was then washed four times and the powder dried at 110 °C overnight. Finally, it was calcined at 600 °C for 8 h under flowing air to remove the organic template. The protonated SSZ-13 obtained was denoted as SSZ-13-*x*, where *x* represents the molar ratio of Si/Al from the designated formulation.

In this work, the hybrid catalyst $In_2O_3$/SSZ-13-*x* was prepared by the granular mixing of the two ingredients. This approach was taken to avoid the migration and interference of indium ions in the zeolite catalyst, which has been found to reduce the performance of the zeolites when the components are mixed by methods allowing more intimate contact between the materials.[31] Prior to this, each component powder was pelletized individually on a Specac Manual Hydraulic Press (20 mm pellet die, 2.5 tons of pressure) before being crushed and then sieved into the granular sizes required (250−500 μm). The resulting granular ingredients were mixed well in a glass vial by shaking. The mass ratio of the $In_2O_3$ oxide and SSZ-13 zeolite components was fixed at 2:1 ($m_{oxides}/m_{zeolites}$ = 2:1) in this work.

**2.2. Characterization of the Catalyst.** The powder X-ray diffraction (PXRD) patterns of the as-synthesized samples were recorded on a Bruker D8 X-ray diffractometer with Cu K$\alpha$ ($\lambda$ = 1.54 Å), using radiation within a scanning angle of 2$\theta$ from 5 to 55° (step size 0.029°, dwell time 1 s).

The morphology and size of the zeolite particles were analyzed by scanning electron microscopy (SEM) using a JEOL JSM-7800F Prime scanning electron microscope.

Element analysis was carried out on an Axios wavelength dispersive X-ray fluorescence (XRF) spectrometer (Zetium, Malvern-Panalytical) employing a Rh anode as the X-ray source. Qualitative and quantitative analyses were carried out using the Super Q software package and a set of OMNIAN calibration samples provided by Malvern-Panalytical (Malvern, U.K.).

The specific surface area and pore size distribution tests were measured by $N_2$ adsorption at −196 °C on a Micromeritics Tri-Star 3000 instrument. Samples were degassed at 300 °C for 6 h prior to testing; Brunauer−Emmett−Teller (BET) surface areas were calculated using the Brunauer−Emmett−Teller (BET) equation based on fitting the data in the relative pressure ($P/P_0$) range from 0.005 to 0.05, and the *t*-plot method was used to determine the micropore volumes.

Temperature-programmed desorption of ammonia ($NH_3$-TPD) was performed to obtain the acid density of the zeolite sample by following an analogous procedure described by Arora et al.[18] In a flow apparatus comprised of a versatile feed system and a quartz tube reactor (4 mm inner diameter), 30 mg of calcined sample (250−500 μm) was treated by flowing 2000 ppm of $NH_3$/Ar with a total flow rate of 20 N mL/min at 100 °C for 2 h until saturation was reached, followed by an Ar (20 N mL/min) flow for 4 h to remove physiosorbed $NH_3$. Then, TPD was conducted in pure Ar (20 N mL/min) flow with a ramping rate of 10 °C/min to reach a final temperature of 700 °C. The effluent streams were monitored by online mass spectrometry (Hiden HPR-20 QUI MS), and the $NH_3$ signal was recorded at $m/z$ = 17. MS signals were calibrated prior to the experiment using gas mixtures of a known composition.

**2.3. Reaction Testing and *In Situ* Precoking Treatment.** The catalytic reaction and the *in situ* precoking treatment were carried out in a stainless-steel fixed bed reactor (VINCI Technologies, France) with an inner diameter of 8.3 mm and a length of 215 mm. Typically, 1 g of well-mixed hybrid catalyst ($m_{oxides}/m_{zeolites}$ = 2:1) was placed in the isothermal zone of the reactor tube, and the empty volume at the top and bottom of the catalyst bed was filled with silicon carbide (Sigma-Aldrich, 500 μm). The interfaces between the silicon carbide and catalyst were separated by quartz wool plugs. The reaction temperature was monitored by a K-type thermocouple that was inserted in the middle of the catalyst bed while the reaction pressure was controlled automatically by a pneumatic back pressure valve.

In the case of fresh hybrid catalysts, these were pretreated prior to the reaction in a pure Ar flow (150 N mL/min) at 400 °C for 1 h before being cooled to the desired reaction temperature (325−400 °C). The reactant gases with the correct ratio of $H_2/CO_2$ were then introduced into the reactor before increasing to the target pressure (10−40 bar) for the $CO_2$ hydrogenation reaction.

*In situ* precoking refers to the modification of the catalyst with coke by applying a transient temperature treatment of the catalyst. When the fresh hybrid catalysts had reached 400 °C, under atmospheric pressure in Ar, a mixture of $CO_2$ (15.2 N mL/min) and $H_2$ (91.4 N mL/min) gases was fed to the reactor at a total pressure of 30 bar and kept constant during the whole treatment. First, the initial treatment (30 bar, 400 °C) was maintained for 0 or 5 h. Then, the temperature was decreased to 325 °C and a second stage of the treatment was conducted (30 bar, 325 °C) for 10−20 h. Finally, the temperature was increased to 400 °C at 30 bar under the fixed reactant atmosphere, followed by a 5 h dwelling time to complete one cycle of a precoking treatment. After the precoking treatment, the catalyst bed was first


https://doi.org/10.1021/acs.energyfuels.3c03172
Energy Fuels XXXX, XXX, XXX−XXX

adjusted to the reaction temperature under atmospheric pressure, and then the reaction was carried out under the target pressure.

All effluents were analyzed using an online gas chromatograph (GC-456, Bruker). This was equipped with a Molsieve 5 Å column (1 m × 3.175 mm) connected to a thermal conductivity detector for the detection of permanent gases and methanol and a BR-Swax column (30 m × 320 $\mu$m × 1 $\mu$m) connected to a flame ionization detector for the analysis of hydrocarbons. The identification and quantification of each gaseous compound ($CO_2$, CO, $CH_4$, $CH_3OH$, DME, and $C_1$ to $C_7$ hydrocarbons) were performed based on the retention times obtained and the calibration factors acquired from gas calibration standards (Linde Gas). The $CO_2$ conversion, along with CO and hydrocarbon selectivity and yield, was calculated based on the following equations

$$\text{CO}_2\text{ conversion: conv. CO}_2 = (n_{\text{CO}_2,\text{in}} - n_{\text{CO}_2,\text{out}})/n_{\text{CO}_2,\text{in}} \times 100\% \quad (1)$$

$$\text{CO selectivity: sel. CO} = n_{\text{CO}}/(n_{\text{CO}_2,\text{in}} - n_{\text{CO}_2,\text{out}}) \times 100\% \quad (2)$$

$$\text{CH}_3\text{OH selectivity: sel. MeOH} = n_{\text{MeOH}}/(n_{\text{CO}_2,\text{in}} - n_{\text{CO}_2,\text{out}}) \times 100\% \quad (3)$$

$$\text{DME selectivity: sel. DME} = 2 \times n_{\text{DME}}/(n_{\text{CO}_2,\text{in}} - n_{\text{CO}_2,\text{out}}) \times 100\% \quad (4)$$

$C_nH_m$ selectivity among hydrocarbons without CO, $CH_3OH$, and DME:

$$\text{sel. C}_n\text{H}_m = n \times n_{\text{C}_n\text{H}_m}/(n_{\text{CO}_2,\text{in}} - n_{\text{CO}_2,\text{out}} - n_{\text{CO}} - n_{\text{MeOH}} - 2 \times n_{\text{DME}}) \times 100\% \quad (5)$$

$$\text{yield of CH}_3\text{OH in effluent: yield MeOH} = (n_{\text{MeOH}}/n_{\text{CO}_2,\text{in}}) \times 100\% \quad (6)$$

$$\text{yield of C}_n\text{H}_m\text{ in effluent: yield C}_n\text{H}_m = n \times (n_{\text{C}_n\text{H}_m}/n_{\text{CO}_2,\text{in}}) \times 100\% \quad (7)$$

$$\text{total yield of light olefins: total yield } C_2^{=} - C_4^{=} = \text{yield } C_2H_4 + \text{yield } C_3H_6 + \text{yield } C_4H_8 \quad (8)$$

where $n_{\text{CO}_2,\text{in}}$: inlet moles of $CO_2$, $n_{\text{CO}_2,\text{out}}$: outlet moles of $CO_2$, $n_{\text{CO}}$: outlet moles of CO, $n_{\text{MeOH}}$: outlet moles of MeOH, $n_{\text{DME}}$: outlet moles of DME, and $n_{\text{C}_n\text{H}_m}$: outlet moles of hydrocarbon.

$n_{\text{CH}_4}$, $n_{\text{C}_n^0}$, and $n_{\text{C}_n^=}$ are the outlet moles of methane, paraffins, and olefins, respectively. An evaluation of the Weisz−Prater criteria (details in Tables S1 and S2) at the highest temperature conditions for the $CO_2$ reaction rate on $In_2O_3$ and the methanol reaction rate on SSZ-13 indicated that pore transport resistance could be neglected under the conditions used in this study.

**2.4. Analysis of Coke Confined over Spent Catalysts.** Before being discharged from the reaction tube, all spent catalysts were purged thoroughly with a continuous flow of argon (50 N mL/min) at 110 °C overnight and then collected at room temperature. Each obtained spent catalyst sample was uniformly ground and mixed before analysis. As a result, the analysis of the coke on the spent catalysts represents the average results for the entire catalyst bed.

The total amount of coke retained over the spent catalysts was measured by a thermogravimetric analyzer TGA/DSC 3+ (Mettler Toledo). A 10 mg sample of the used catalyst was packed in an alumina crucible and heated from 30 to 700 °C with a ramping rate of 10 °C/min in an air flow of 100 N mL/min. The weight loss of the spent zeolite catalyst between 300 and 700 °C was used to estimate the content of coke.[19] Here, the final amount of coke deposited on the spent hybrid catalyst was estimated from the weight loss of the spent catalyst in the temperature range of 300−700 °C minus the weight loss of the fresh hybrid catalyst in the same temperature range. The TGA patterns of coke in all samples are normalized based on that starting point at 300 °C.

The nature of the confined soluble coke was analyzed qualitatively according to the method described by Bhawe et al.[32] Typically, 300 mg of spent catalyst powder ($m_{\text{oxides}}/m_{\text{zeolites}}$ = 2:1) was placed in a 15 mL Teflon vessel fitted with a cover, after which 2 mL of hydrofluoric acid solution (48 wt % in aqueous phase) was added to dissolve it carefully. Upon the complete digestion of the zeolite framework (after 30 min), the organic species released were extracted by adding 5 mL of dichloromethane ($CH_2Cl_2$). The extracted products were then filtered using a 0.45 $\mu$m nylon membrane filter and collected for GC-MS analysis. One microliter of the liquid sample was injected into an Agilent GC system 7890B coupled with an Agilent 5977A mass spectroscopy (MS) detector equipped with a moderately polar VF1701 ms column (30 m × 0.25 mm × 0.25 $\mu$m). The injector port temperature was set at 280 °C (isothermal), and the oven temperature was ramped up from 40 to 280 °C at a rate of 10 °C/min and held for 10 min at the highest temperature. The total ion current (TIC) chromatograms of the GC-MS data were obtained *via* automatic scanning in the mass-to-charge ratio ($m/z$) range from 40 to 300.

Considering that there are still some carbonaceous species that are difficult to dissolve in $CH_2Cl_2$, such as graphitized coke or polycyclic aromatics with a high C/H ratio (mole ratio of carbon to hydrogen), temperature-programmed oxidation (TPO) was used to characterize the oxidative decomposition of the total coke species and analyze their C/H ratio. During TPO experiments, the consumption of $O_2$ was continuously monitored, as well as the emissions of CO, $CO_2$, and $H_2O$ during the oxidative decomposition of the coke. In brief, 50 mg of spent catalyst was placed in a quartz tube reactor and pretreated at 110 °C in flowing Ar for 1 h prior to oxidation. Then, 5000 ppm of the $O_2$/Ar flow, with a total flow rate of 20 N mL/min, was introduced into the tube reactor at room temperature before the temperature of the sample was increased from 25 to 700 °C, with a ramping rate of 10 °C/min and held at 700 °C for 2 h so that all organic coke was fully decomposed. The mass spectra of $O_2$, CO, $CO_2$, and $H_2O$ were calibrated using a gas mixture of known composition.

Diffuse reflectance infrared Fourier transform spectra (DRIFTS) were recorded to ascertain the change in the acidity of the hybrid catalysts before and after the reaction. By employing a Vertex70 spectrometer equipped with a mercury cadmium telluride (MCT) detector, an amount (~15 mg) of sample powder was packed in a high-temperature reaction cell (Harrick Praying Mantis) equipped with a $CaF_2$ window. After pretreatment at 550 °C for 60 min under 100 N mL/min of Ar flow, the sample was protected by Ar flow while cooling down to 30 °C for measurement. Then, 1000 ppm of continuous $NH_3$/Ar flow (100 N mL/min) was dosed gradually into the cell while the synchronous adsorption spectra were recorded in the range of 4000−1000 $cm^{-1}$ with a resolution of 4 $cm^{-1}$ until the sample reached saturation, which was confirmed by a mass spectrometer (Hiden HR20) connected to the outlet stream of the cell. After adsorption at 30 °C, the sample was heated to 200 °C under Ar flow for desorption and then cooled down to 30 °C for spectra collection.

## 3. RESULTS AND DISCUSSION

**3.1. Properties of Synthesized SSZ-13 Zeolites.** Using a composition range yielding Si/Al ratios from 15 to 25, SSZ-13 zeolites were successfully synthesized using TMAdaOH as the sole SDA in the hydroxide media. This method has been suggested by Di Iorio et al. to predominantly produce isolated proton sites within SSZ-13.[30] The synthesis method of SSZ-13 zeolites used in this study has been discussed in one of our other works.[33] The powder X-ray diffraction (XRD) patterns


https://doi.org/10.1021/acs.energyfuels.3c03172
Energy Fuels XXXX, XXX, XXX−XXX

**Table 1. Physicochemical Information of Fresh SSZ-13 Zeolites**

| sample | Si/Al[a] ratio | $S_{BET}$[b] ($m^2/g$) | $V_{meso}$[c] ($cm^3/g$) | $V_{micro}$[d] ($cm^3/g$) | particle size[e] ($\mu m$) | crystal shape | Brønsted acidity[f] ($mmol/g_{cat}$) |
|---|---|---|---|---|---|---|---|
| SSZ-13-15 | 14.2 | 617.7 | 0.056 | 0.26 | 2.73 | pseudocube | 0.35 |
| SSZ-13-20 | 20.3 | 578.3 | 0.059 | 0.24 | 2.88 | cube | 0.25 |
| SSZ-13-25 | 27.3 | 514.8 | 0.051 | 0.22 | 2.84 | cube | 0.23 |

[a]Mole ratio determined by XRF. [b]BET surface areas measured from $N_2$ adsorption isotherm using the BET method. [c]Mesopore volume measured from $N_2$ adsorption isotherm using the BJH method. [d]Micropore volume measured from $N_2$ adsorption isotherm using the *t*-plot method. [e]Average crystal particle size estimated from SEM micrographs. [f]Brønsted acid density accessed from the deconvolution peaks of the $NH_3$-TPD curve with centers ranging from 300 to 700 °C.

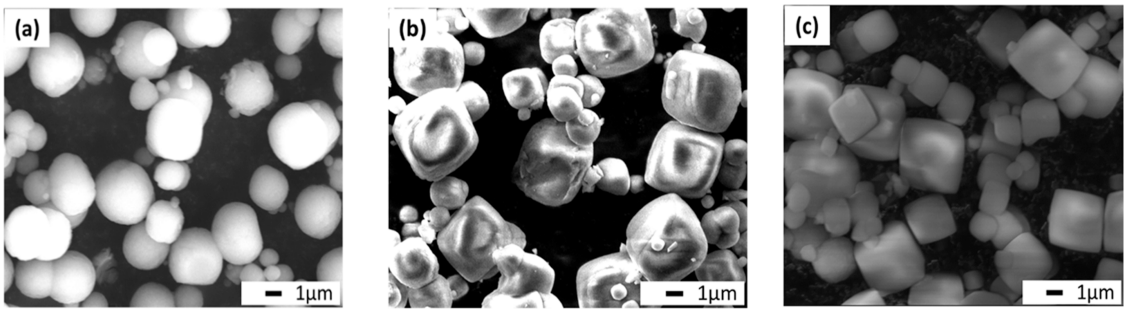


**Figure 1.** SEM images of SSZ-13 zeolite samples: (a) SSZ-13-15, (b) SSZ-13-20, and (c) SSZ-13-25.

confirmed that all obtained zeolite samples exhibited a fully crystalline CHA phase, while $N_2$ adsorption−desorption isotherms showed the typical isotherms of microporous zeolites, and their corresponding micropore volumes were around 0.24 $cm^3/g$. The XRD patterns, along with other details, are shown in our earlier study.[33] However, increasing the Si/Al mole ratio (SAR) resulted in a change in the diffraction peak intensity. Given that the XRD characteristic peak areas obtained under the same test conditions can be used to compare the relative crystallinity of zeolites,[34] these weakened peak areas indicated a decrease in crystallinity of the SSZ-13 zeolites with increasing Si/Al mole ratio during crystallization. Besides, a change in the relative areas of the main diffraction peaks (9.66, 20.87°) in the XRD pattern may be attributed to the emergence of a different preferential growth structure in the crystal.[35] These results are also in good agreement with the decreased BET surface (617.7−514.8 $m^2/g$) and varied crystal morphologies shown in Table 1. The SEM image of the SSZ-13-15 sample in Figure 1 showed pseudocubic crystal particles with rounded edges, while those of SSZ-13-20 and SSZ-13-25 were more cubic but of a similar average size. In the crystallization of SSZ-13 zeolite, the mature crystals always show cubic crystal faces.[35] The precursor solutions of the samples with lower SAR contained more $[AlO_4]^-$ tetrahedrons and crystallized more slowly into well-defined cubic phase crystals compared with the ones with higher SAR. Therefore, within the fixed synthesis time used, their degree of ripening was lower, and the pseudocubic crystals with rounded edges were formed, as evident for samples SSZ-13-15 and SSZ-13-20.

The $NH_3$-TPD results (displayed in our earlier study[33]) showed that all samples presented two major desorption peaks centered around ∼200 and 440 °C, which correspond to weak and strong acid sites, respectively. Typically, the adsorption of $NH_3$ on strong acid sites (peak range above 300 °C) is often used to measure the density of Brønsted acid sites (BAS), as reported elsewhere.[18,33,36] This BAS density, calculated using deconvolution and integration of the desorption peaks with centers ranging from 300 to 700 °C,[33,36] is given in Table 1. With an increase in the ratio of Si/Al, the BAS density decreased gradually, giving an order of the acid densities for the SSZ-13 zeolite samples to be SSZ-13-15 > SSZ-13-20 > SSZ-13-25.

**3.2. Effect of Temperature on Reactivity and Coke Modification.** Previous work by the current authors found, from both equilibrium calculations and experiments, that temperature plays a crucial role in the conversion of $CO_2$ and the selectivity for products over bulk $In_2O_3$ catalysts.[37] It was observed that methanol synthesis and the RWGS reaction are parallel and competitive during $CO_2$ hydrogenation and, because $CO_2$ to methanol is an exothermic reaction while RWGS is endothermic, higher temperature favors higher selectivity for CO from both thermodynamic and kinetic aspects.[5] More specifically, these previous tests showed that the selectivity for methanol was reduced to less than 1.3% on the $In_2O_3$ catalysts at a reaction temperature above 400 °C.[37] In addition, the reaction temperature has a significant effect on the MTO reaction. The coupling reaction of C−C bonds can only be carried out above 300 °C, and the optimum reaction temperature of the conventional MTO process is between 400 and 450 °C over the SAPO-34 zeolite. Too high or too low reaction temperature will cause rapid coking of the catalyst and lead to deactivation.[12] Moreover, the temperature also affects water production from $CO_2$ hydrogenation, thereby also affecting catalyst lifetime and hydrocarbon product selectivity. As water is produced in both the methanol synthesis and RWGS processes, promoting $CO_2$ conversion by increasing the reaction temperature can also cause the concentration of water to increase in the effluent.[5] Many articles have disclosed that $H_2$ and water contribute significantly to improving the lifetime of zeolite/zeotype catalysts.[16−22] In addition, CO[38] and water[19,39] might affect the selectivity for olefins in the process of converting methanol to olefins over zeolites. However, none of the reports has explored the overall effects of temperature on the performance of zeolites during the conversion of $CO_2$ to olefins.

In the present study, the influence of the reaction temperature was first evaluated over the hybrid catalyst of


https://doi.org/10.1021/acs.energyfuels.3c03172
Energy Fuels XXXX, XXX, XXX−XXX

**Table 2. Normalized Yield and Lifetime over the Hybrid Catalyst of $In_2O_3$ and SSZ-13-25 under Varied Reaction Conditions**

| temperature (°C) | total pressure (bar) | $H_2$ partial pressure[a] (bar) | $CO_2$ conversion (%) | intermediate methanol or methanol feeding capacity ($g_{MeOH}/h/g_{zeolite}$)[b] | lifetime[c] (h) |
|---|---|---|---|---|---|
| 400 | 30.0 | 25.7 | 45.5 | 0.41−0.43 | >20.0 |
| 375 | 30.0 | 25.7 | 40.7 | 0.41−0.47 | >20.0 |
| 350 | 30.0 | 25.7 | 26.8 | 0.19−0.33 | 9.0 |
| 325 | 30.0 | 25.7 | 16.7 | 0.19−0.23 | 4.0 |
| 325 | 40.0 | 34.3 | 17.3 | 0.23−0.27 | 2.5 |
| 325 | 20.0 | 17.1 | 17.4 | 0.17−0.24 | 6.5 |
| 325 | 10.0 | 8.6 | 15.2 | 0.14−0.16 | >20.0 |
| 400 | 0.1 | 0 | | 0.50 | 4.8[40] |
| 375 | 0.1 | 0 | | 0.50 | 2.5[40] |
| 350 | 0.1 | 0 | | 0.50 | 2.4[40] |
| 325 | 0.1 | 0 | | 0.50 | 1.2[40] |

[a]Hydrogen partial pressure is zero under pure MTO reaction conditions without hydrogen. [b]Methanol capacity is calculated from the total moles of carbon atoms in hydrocarbons and unconverted methanol in the effluent during the observed lifetime, where it is assumed that all hydrocarbon products are generated from intermediate methanol. [c]Lifetime of the catalyst is determined by the time interval between the start of feeding to the first detection of unconverted methanol in the reactor effluent.

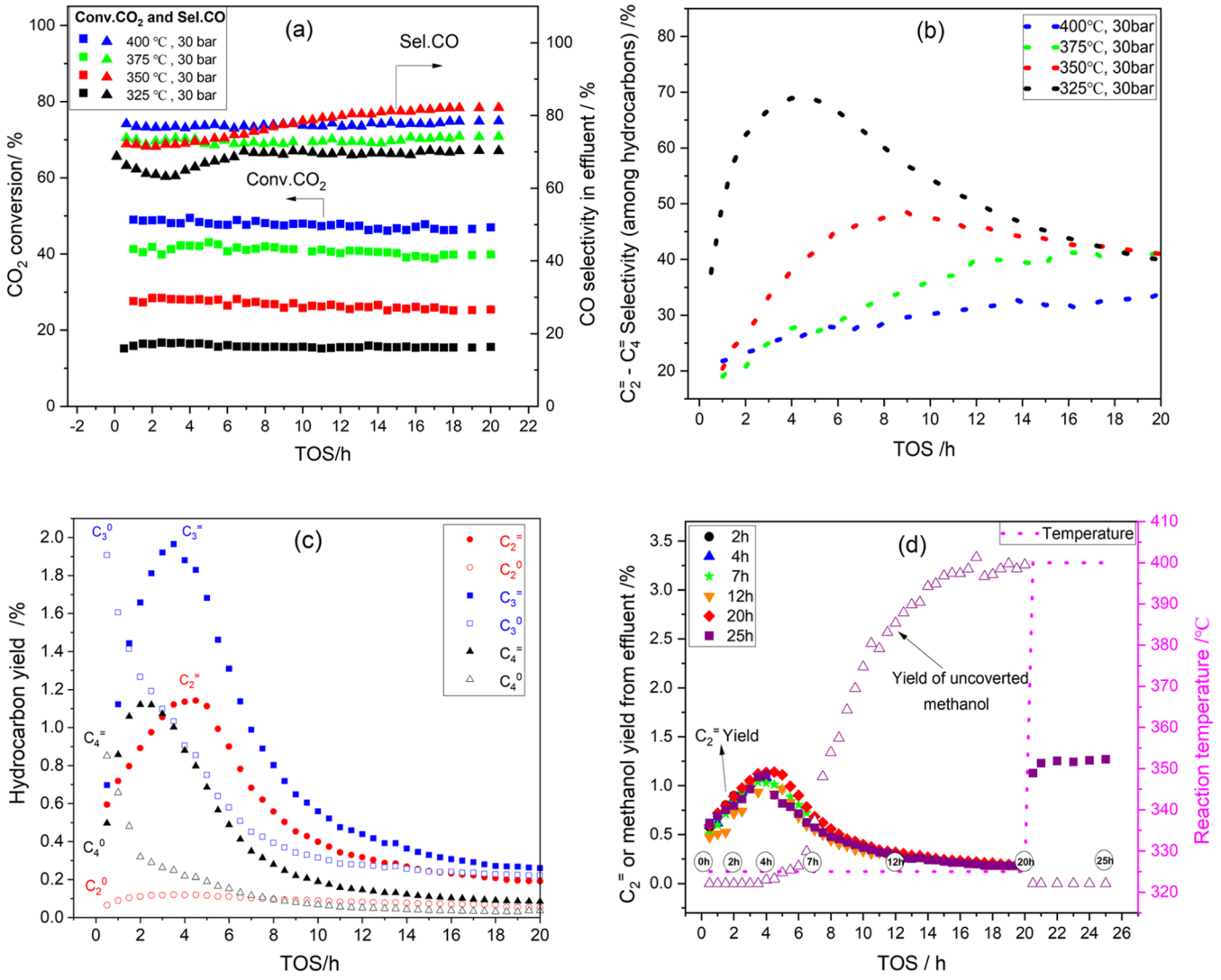


**Figure 2.** Catalytic performance of $CO_2$ hydrogenation over $In_2O_3$/SSZ-13-25 at different temperatures and as a function of time-on-stream (TOS). (a) Conversion of $CO_2$ and selectivity for CO. (b) Selectivity for light olefins (based on total hydrocarbons). (c) Yield of major hydrocarbons at 325 °C. (d) Ethylene and methanol yields during the temperature transient experiment. In the transient experiment, the times 2, 4, 7, 12, and 20 h indicate that the reaction was carried out at 325 °C for these respective time periods. The time 25 h means that the reaction was first conducted at 325 °C for 20 h and then at 400 °C for 5 h. Other conditions: catalyst weight = 1 g; weight ratio of $In_2O_3$/SSZ-13-25 = 2 in granule mixture; GHSV = 6400 N mL/(g h); $P$ = 30 bar; and $H_2/CO_2$ = 6.


https://doi.org/10.1021/acs.energyfuels.3c03172
Energy Fuels XXXX, XXX, XXX−XXX

$In_2O_3$ and the SSZ-13-25 zeolite with respect to the distribution of hydrocarbons and the formation of coke during $CO_2$ hydrogenation. A temperature range of 400−325 °C was chosen for all experiments under a pressure of 30 bar and an hourly space velocity for the gas of 6400 N mL/(g h) to match the methanol synthesis and MTO reaction.[5,37] In the hybrid catalyst process, methanol is not directly fed to react over SSZ-13 zeolite but only exists as an intermediate produced by the methanol synthesis catalyst component (indium oxide catalyst). To compare the MTO performance of SSZ-13 zeolite at different temperatures during $CO_2$ hydrogenation, the sum of the yields of all hydrocarbons and unconverted methanol were normalized as the calculated methanol capacity in Table 2, according to the method as described by Nieskens et al.[16]

The conversion of $CO_2$ and the distributions of the main product *versus* time-on-stream (TOS) are given in Figures 2 and S1. It should be noted that the selectivity for different hydrocarbons (HCs) is based on total HCs, not including CO. At higher temperatures, the concentrations of the light olefins (Figures 2b and S1) were more stable, showing that a high temperature is beneficial for the stability of the catalysts. The reason for the lower stability at low temperatures is mainly due to the zeolite component since the indium oxide catalyst is highly stable under these experimental conditions, as the results of our previous work have shown.[33,37] The decreasing hydrocarbon yields with TOS were always accompanied by an increasing methanol breakthrough, which can be attributed to deactivation of the zeolite component during the reaction, as can be seen in Figure S1. At 375 and 400 °C, the catalyst was stable for more than 20 h. However, when the temperature was decreased from 350 to 325 °C, the lifetime of the catalyst (defined as the time before methanol breakthrough) was reduced from 9 to 4 h. For the pure MTO reaction over SSZ-13 zeolite described by Borodina,[40] the lifetime of SSZ-13 at 325 and 400 °C was only about 1.2 and 4.8 h, respectively. However, in our case, with a similar methanol feeding capacity (0.5 $g_{MeoH}/h/g_{zeolite}$) and at the same temperature, the stability of the SSZ-13 zeolite in $CO_2$ hydrogenation is longer than 20 h. Thus, the stability is more than 4 times higher compared with that of the pure MTO reaction in the literature. At 325 °C, the lifetime of our catalyst was 4 h, which is 2.9 times longer than for the pure MTO reaction in the literature.

However, it should be noted that the lifetime of a catalyst varies not only with temperature but also with, for example, pressure and feed concentration. The longer lifetime in our experiments is likely mainly attributed to the effects of hydrogen on the MTO reaction, where it has been speculated that the hydrogen and hydrogenation reactions have the positive ability to prevent the hydrogen transfer reaction or formaldehyde-mediated paths from generating heavy aromatics.[18] Moreover, the increased $CO_2$ conversion at higher temperatures produces more water, resulting in a greater synergistic effect of water than pure hydrogen, thereby inhibiting the formation of heavy coke. This increased lifetime of catalysts in MTO reactions under a hydrogen and water atmosphere was also discussed by Zhao et al.[19] However, with the decrease of the reaction temperature, the hydrogenation rate decreases and the water content also decreases due to the lower $CO_2$ conversion rate, which leads to weakening of the coke inhibition reaction by water and hydrogen, so the SSZ-13 zeolite appears to rapidly deactivate as also is found under pure MTO reaction conditions.

The temperature not only affects the CO selectivity over the indium oxide catalyst but also affects the synergistic effect of indium oxide and zeolite, which also causes a further change in the selectivity for CO. The RWGS reaction is both thermodynamically and kinetically favorable at high temperatures; thus, the higher reaction temperature promotes selectivity for CO over the $In_2O_3$ catalyst.[5,33,37] Previous work has demonstrated that the suppression of the RWGS reaction could occur in hybrid catalyst systems when introducing zeolite to convert methanol to hydrocarbon. The use of a bifunctional catalyst ($In_2O_3$/ZSM-5) reduced the CO selectivity significantly compared with the use of $In_2O_3$ alone due to a favorable equilibrium driving force.[33,41] Therefore, the selectivity for CO is also affected by the activity of the zeolites, even though the zeolite is not responsible for $CO_2$ activation. The reaction temperature indirectly affects the selectivity for CO by changing the activity of the zeolite during the hydrogenation of $CO_2$ to olefins. In Figure 2a, when the hybrid catalyst was operated at 325 °C in the initial stage (TOS < 2 h), fewer hydrocarbon pool species (HCP) were generated to convert methanol efficiently, so suppression of RWGS was weaker and CO selectivity was higher. When the accumulation of HCP and coke gradually increased, and the methanol conversion capacity changed from high to low, the CO selectivity showed a downward trend followed by an upward trend. At 375 and 400 °C, the zeolite catalyst was active, and the CO selectivity tended to be stable as the reaction proceeded, at 73 and 77%, respectively.

Temperature also affects the distribution of hydrocarbons, as well as the olefin/paraffin ratio, during $CO_2$ hydrogenation reactions, as seen in Figure 2b. Higher selectivity for light olefins (total $C_2$−$C_4$ olefins) was obtained at a lower temperature, which increased rapidly as the reaction progressed before deactivation. The lower the temperature, the faster the growth rate of the olefin selectivity. The highest selectivity for light olefins was 70% (based on total hydrocarbons), which was achieved at 325 °C at a TOS of 4 h. However, for the reaction at 400 °C, the selectivity of light olefins was just 32.6% after the reaction was run for 20 h. Figure 2c shows in more detail the distribution of light hydrocarbon products ($C_2$−$C_4$) for the reaction at 325 °C. It is worth noting that the yields of ethylene and ethane exhibited a similar trend with TOS, whereas the $C_{2+}$ alkenes (e.g., propene and butene) and their corresponding alkanes (e.g., propane and butane) showed opposite trends before deactivation that became the same during deactivation. It has generally been assumed that the formation of ethylene is related closely to the aromatic cycle, the accumulation of the hydrocarbon pool species (active coke), and that steric hindrance would be of help in improving the selectivity for ethylene.[12−14] It was also confirmed by the TGA results that the high production of ethylene (Figure 2b) was correlated with a certain amount of coke formation (Figure S2). Thus, the more coke deposited on the catalyst without deactivation, the higher the selectivity for $C_2$. In contrast, the formation of $C_{2+}$ alkenes primarily follows the coke-independent olefin cycle route.[12−14] The initial propylene and butene generated on the acid sites of the zeolite are further hydrogenated and converted to propane or butane on the same site under a hydrogen atmosphere. Therefore, in the initial stages of the reaction, when the hydrocarbon pool species and coke accumulation were low, $C_{2+}$ alkanes rather than their corresponding alkenes were dominant among hydrocarbon products. However, the


https://doi.org/10.1021/acs.energyfuels.3c03172
Energy Fuels XXXX, XXX, XXX−XXX

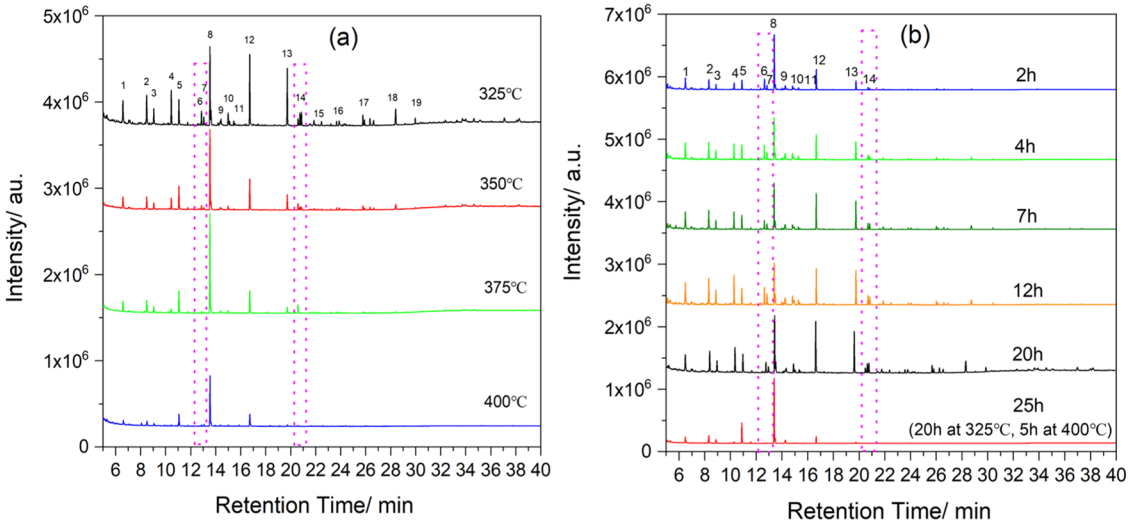


**Figure 3.** GC-MS results of the soluble coke species retained in the spent catalysts after the reaction at different temperatures and TOS. (a) After 20 h of reaction at 325−400 °C. (b) After 2−20 h at 325 °C and after 20 h at 325 °C followed by 5 h at 400 °C (total 25 h). 1: toluene; 2 and 3: xylene; 4 and 5: trimethylbenzene; 6: butyl-adamantane; 7: dimethyl-adamantane; 8 and 9: tetramethylbenzene; 10 and 11: naphthalene; 12: pentamethylbenzene; 13: hexamethylbenzene; 14: methyl-diadamantane; 15: trimethyl-naphthalene; 16: tetramethyl-naphthalene; 17: naphthalene; 18: 2,6-diisopropylnaphthalene; and 19: dimethylphenanthrene. More detailed identifications of soluble coke species can be seen in Table S4.

accumulated coke over the catalyst can also affect the hydrogenation of $C_{2+}$ alkenes as the reaction proceeds. Typically, as coke accumulation increased, the selectivity for propane and butane gradually decreased, while the selectivity for propylene and butene gradually increased (seen in Figure 2c). DeLuca et al. claimed that the hydrogenation barrier of alkene decreased as the chain length of the molecule increased and its corresponding carbonium species stabilized.[20] Compared with propylene and $C_{3+}$ olefins, it was difficult for ethylene to hydrogenate over a weak acid site. The yield of ethane was therefore low and showed a trend similar to that of ethylene. However, the yield of propylene increased gradually as the yield of propane decreased, while the total yield of $C_3$ hydrocarbons remained almost unchanged with time prior to deactivation. The same trend for the hydrocarbon distributions can also be seen at temperatures of 400 and 375 °C (Figure S4). These results indicated that suppressed hydrogenation facilitated the production of more propylene and $C_{3+}$ olefins rather than their corresponding paraffins. The successive deposition of hydrocarbon pool species and coke inhibits $C_{2+}$ olefin hydrogenation, causing the total selectivity for olefins to increase gradually as the reaction progresses until deactivation begins to dominate.

Considering that the synergistic effects of hydrogen and water could greatly reduce the coking precursors or coke accumulation at high temperatures, the *in situ* treatment of the catalyst was investigated in a temperature transient experiment. In this experiment, the hybrid catalyst was first operated at a low temperature of 325 °C for 20 h until it was deactivated, and thereafter, when keeping the other reaction conditions unchanged, the reaction temperature was raised to 400 °C for 5 h. The changes of ethylene and unreacted methanol in the effluent with reaction time (TOS) are recorded, as shown in Figure 2d. During the run for 20 h at 325 °C, the results clearly showed that the catalyst was gradually deactivated. However, the activity of the deactivated catalyst was recovered well just by changing the reaction temperature from 325 to 400 °C since the production of olefins was restored and no unconverted methanol was in the effluent. A more detailed comparative experiment showed that the yield of ethylene was higher for the regenerated catalyst compared to the fresh catalyst under the same conditions (Figure S5). This reveals that the temperature treatment also plays an important role in modifying the active sites of the catalyst. A similar phenomenon was also found by Nieskens et al. for hybrid catalysts (CuZnAl oxides and SAPO-34) used in converting syngas to hydrocarbons, where they reported that the coke formed at 300 °C could be removed completely by increasing the temperature to 410 °C. This was explained by speculation that the type of coke might be different from that formed traditionally during a pure MTO reaction.[16] However, no further exploration was conducted into this phenomenon.

After the reaction at different temperatures (catalytic performance in Figure 2a,b) and after experiments with varied TOS at 325 °C and the subsequent temperature transient (catalytic performance in Figure 2d), the coke restrained in the spent catalysts was analyzed by GC-MS, TGA, and TPO characterization. Since it is apparent from Figure 2d that the catalytic performance of the catalysts after different TOS at 325 °C is identical at the same TOS, the analysis of these spent catalysts will provide information regarding the evolution of amounts and character of coke species with TOS. The results of TGA indicated that a higher amount of coke was accumulated at lower temperatures (Figure S2) and after a longer operation time (Figure S3). The GC-MS gave the distinct and detailed distribution of soluble coke species after the reaction at different temperatures and TOS, as shown in Figure 3. At 400 °C, virtually all of the soluble coke species were composed of polymethylbenzenes, and most were tetramethylbenzenes. With a decrease in reaction temperature to 325 °C, the relative intensity of heavy polymethylbenzenes (pentamethylbenzene and hexamethylbenzene) increased gradually, and both light adamantane species and heavy polycyclic aromatics began to appear. However, the type of aromatics and their relative distribution seemed to be


https://doi.org/10.1021/acs.energyfuels.3c03172
Energy Fuels XXXX, XXX, XXX−XXX

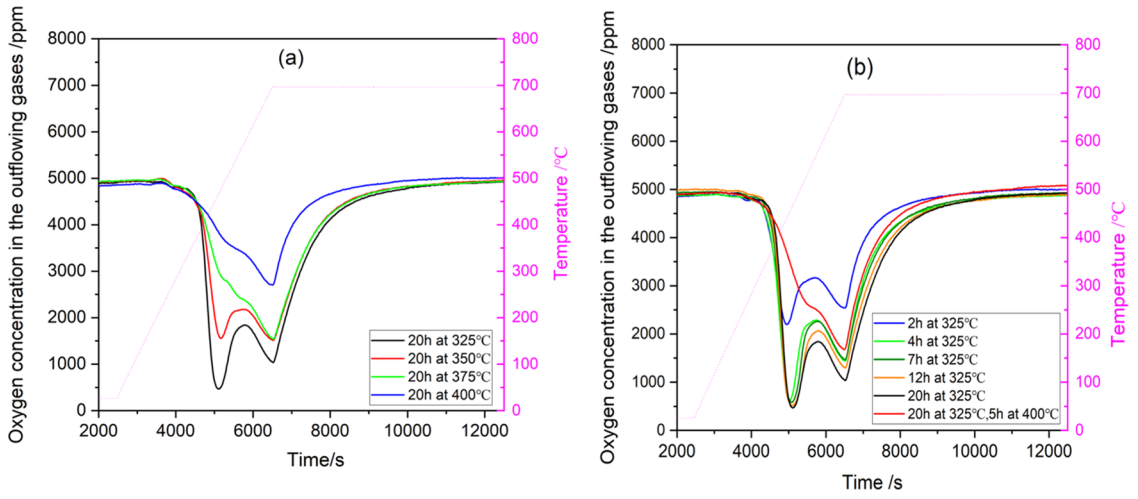


**Figure 4.** TPO profiles of coke deposited on spent catalysts after the reaction at different temperatures or TOS. (a) After 20 h of reaction at 325−400 °C. (b) After 2−20 h of reaction at 325 °C and 20 h at 325 °C followed by 5 h at 400 °C (total = 25 h).

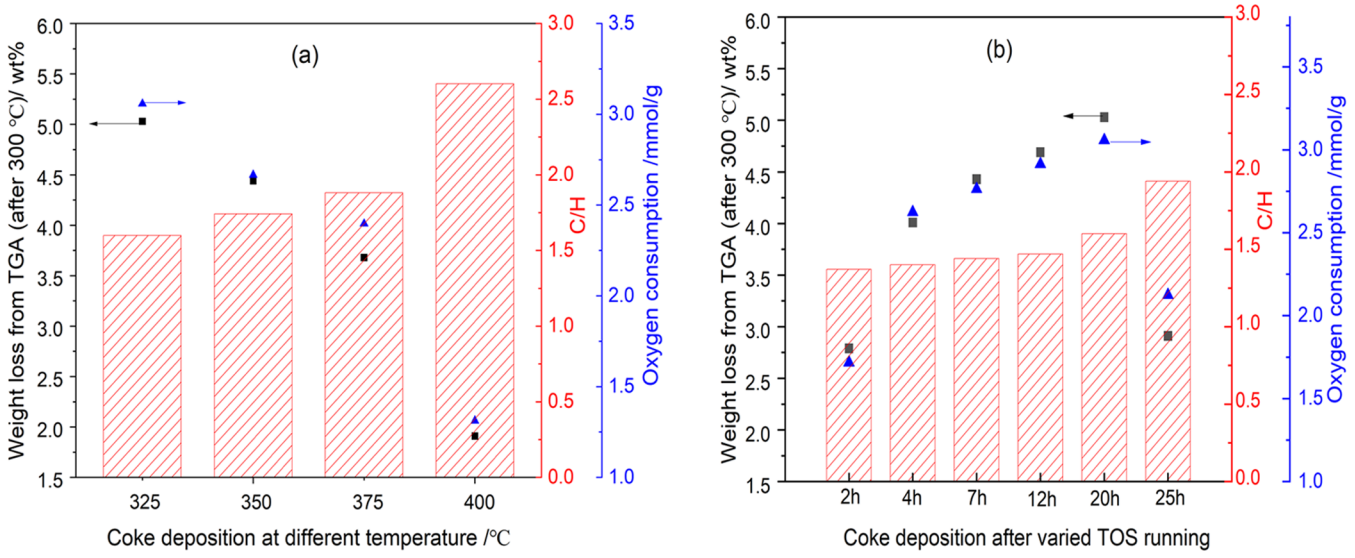


**Figure 5.** Weight loss, oxygen consumption, and quantitative TPO analysis of (C/H mole ratio) of coke deposited within the spent catalysts after the reaction at different temperatures and TOS. (a) After 20 h of reaction at 325−400 °C. (b) After 2−20 h of reaction at 325 °C and 20 h at 325 °C followed by 5 h at 400 °C (total 25 h).

independent of the TOS when the reaction temperature was fixed.

The effect of time (2−20 h) at 325 °C is shown in Figure 3b. The formed species are the same independent of time, but the only difference was that after a shorter time, a lesser amount of coke was observed. Polymethylbenzenes, adamantane, and naphthalene were all present in the spent catalyst after a 2−20 h reaction at 325 °C. It is worth noting here that when the reaction temperature rose to 400 °C after 20 h operation at 325 °C (Figure 3b), the adamantane, heavy polymethylbenzenes, and polycyclic aromatic hydrocarbons disappeared. However, light polymethylbenzenes (toluene to tetramethylbenzene) increased in the recovered catalyst, as shown in Figure 3b. The literature suggests that the hydrocarbon pool species containing light polymethylbenzenes are the main active centers when converting methanol into olefins,[12−14] whereas the adamantane, hexamethylbenzene, and polycyclic aromatics are inactive species that cause the deactivation of the catalyst under different temperature conditions during the MTO reaction. More specifically, deactivation at lower temperatures is mainly associated with the formation of inactive and saturated adamantanes,[12,19,42] whereas, at high temperatures, the formation of heavy polycyclic aromatics (naphthalene, pyrene) plays the main role in deactivation.[12−24,40] Here, fewer inactivate species were present in the form of soluble coke within the spent catalysts after a high-temperature reaction, so the total content was low. This is fully consistent with the reaction results, indicating that a high temperature is favored for stabilizing the catalyst. Most notable is the fact that, unlike in the case of the pure MTO reaction process or MTO without $H_2$ cofeeding, no large numbers of heavy hydrocarbons (such as polycyclic aromatics) were found in the soluble coke from the spent catalyst after $CO_2$ hydrogenation at high temperatures. This difference can be attributed to the inhibition effect water and hydrogen have on the coke condensation, which hinders the accumulation of a large amount of coke.[19] In addition, the low total amount of


https://doi.org/10.1021/acs.energyfuels.3c03172
Energy Fuels XXXX, XXX, XXX−XXX

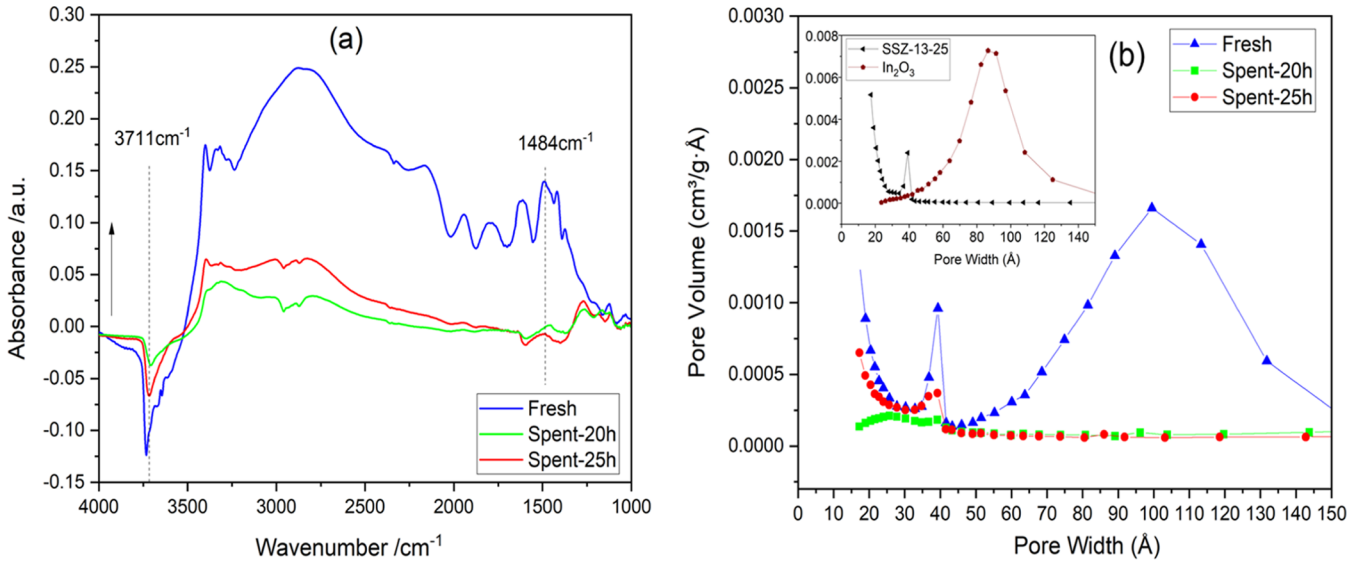


**Figure 6.** Fourier transform infrared (FTIR) spectra of the adsorption of $NH_3$ at 30 °C (a) and pore size distribution analysis (b) of fresh and spent catalysts. The "Fresh" represents an unused catalyst ($In_2O_3$/SSZ-13-25), and the SSZ-13-25 and $In_2O_3$ indicate the zeolite and oxide component, respectively, in the inserted panel of (b). "Spent-20 h" is the spent catalyst after 20 h at 325 °C, and "Spent-25 h" is the spent catalyst after 20 h at 325 °C followed by 5 h at 400 °C.

deposition also limits the detection of trace polycyclic aromatics.

Consistent with the results of GC-MS, the TPO analysis also confirmed that the distribution of coke species and their composition changed drastically with temperature but varied little with the reaction time. The results of Figure 4a indicate that the coke deposited by high-temperature reaction had a main oxygen consumption peak at high temperatures and a weak shoulder peak at low temperatures. With a decrease in reaction temperature, the proportion of the low-temperature oxygen consumption peak gradually increased and became more dominant. More specifically, the coke accumulated after the reaction at 400 °C was mainly decomposed at around 700 °C, and the coke accumulated after the reaction at 325 °C had two distinguishable decomposition peaks centered around ~500 and 700 °C.

These different distributions of coke species with the reaction temperature were also confirmed by the evolution spectra of $CO_2$ and CO during the coke oxidation in Figure S6 and by the quantitative analysis of carbon to hydrogen ratio in coke as shown in Figure 5a. However, when the reaction temperature was fixed at a low temperature (325 °C), the oxidative decomposition profile of coke retained almost the same shape with the progress of the reaction (Figure 4b, 2−20 h). After the reaction at 325 °C for 2 h, although the amount of coke at this time was very low (TGA result from Figure S3), a large proportion of low-temperature oxidative decomposition coke was still present, as shown in Figures 4b and S7. At the same temperature, prolonging the reaction times just gradually accumulated a greater quantity of coke species but did not change their types, which suggests that temperature is the main factor affecting the coke distribution.

In the previous GC-MS analysis, it was found that a low temperature was conducive to the simultaneous formation of light adamantane and heavy polycyclic aromatic hydrocarbons, which are the main causes of the deactivation of catalysts at a low temperature. Here, it is notable that the quantitative TPO results proved that the coke species with a low C/H ratio contributed the most to the deposition of coke at a low temperature. This can be indicated by the oxygen consumption peak at a lower temperature in the TPO profiles of deactivated catalysts, as shown in Figure 4b. Consequently, the more serious the deactivation, the more obvious the oxygen consumption peak at low temperatures. Unlike some heavy polycyclic aromatics or graphitic coke with a high ratio of carbon to hydrogen, characterized as the oxygen consumption peak of concentrated coke at high temperatures,[43] this low-temperature peak in TPO disclosed the formation of light coke in an inactive catalyst. It most likely results from the oxidation of adamantane species with a low composition ratio of carbon to hydrogen, as shown in the GC-MS and quantitative TPO results in Figures 3b and 5b, respectively.

The TPO profile of the regenerated catalyst further confirmed that the light coke, which exhibited the oxygen consumption peak at low temperatures, could be attributed to the inactive adamantane since it can be transformed into active hydrocarbon pool species to recover the activity at higher temperatures as reported for pure MTO reaction conditions.[12] This is illustrated by the fact that after high-temperature regeneration, the catalyst recovered its activity (Figure 2d), and most of the low-temperature oxygen consumption peak of the residual coke disappeared (Figure 4b), but some of the high-temperature oxygen consumption peak was preserved. Combined with the identification results of the GC-MS analysis (Figure 3b, 25 h), these residual coke species are attributed mainly to the light polymethylbenzenes.

The acidity and porous properties of spent hybrid catalysts, as well as fresh hybrid catalysts, were characterized thoroughly by IR spectroscopy and $N_2$ adsorption. In Figure 6a, the IR spectra of adsorbed $NH_3$ at 30 °C were employed to investigate the acidic sites of the hybrid catalysts before and after the reaction in detail. Prior to the adsorption of ammonia, the clean surface of the sample was set as its adsorption baseline. Upon $NH_3$ adsorption, the negative hydroxyl peak at around 3711 $cm^{-1}$ represents the extent to which the surface acidic sites strongly adsorbed ammonia.[33,44] The greater the


https://doi.org/10.1021/acs.energyfuels.3c03172
Energy Fuels XXXX, XXX, XXX−XXX

negative peak, the more ammonia molecules adsorbed on the hydroxyl site, which is reflected by the peaks of stretching vibrations of the strongly adsorbed ammonia molecules at 1484 $cm^{-1}$.[33,44−46] After 20 h of reaction at 325 °C, a large amount of coke accumulated on the spent catalyst, covering the active hydroxyl sites (acid centers) and hindering the diffusion of products by blocking the micropore structure of the catalyst, which led to the serious deactivation as described above. However, both the surface acidity and micropores recovered, to some extent, following the high-temperature (400 °C) treatment without any oxidation treatment (see Figure 6a, 25 h). As shown in Figure 6a, a recovered negative peak of the hydroxyl group (at about 3711 $cm^{-1}$) and a little increased vibration peak of adsorbed $NH_3$ (at about 1484 $cm^{-1}$) confirmed the recovered acidity of the 25 h catalysts (20 h at 325 °C and 5 h at 400 °C). In addition, the increased specific surface area and micropore volume after high-temperature regeneration are also clearly shown in Figure 6b and Table 3, which fully verify the significance of high temperature in restoring catalyst activity.

**Table 3. Textural Properties of Spent and Fresh Catalysts and Their Fresh Ingredients before and after the Reaction**

| sample | $S_{BET}$[a] ($m^2$/g) | $V_{meso}$[b] ($cm^3$/g) | $V_{micro}$[c] ($cm^3$/g) |
|---|---|---|---|
| fresh (SSZ-13-25) | 514.8 | 0.051 | 0.220 |
| fresh ($In_2O_3$) | 95.9 | 0.310 | 0.022 |
| fresh ($In_2O_3$/SSZ-13-25) | 197.7 | 0.120 | 0.073 |
| spent-20 h (20 h at 325 °C) | 21.2 | 0.049 | 0.003 |
| spent-25 h (20 h at 325 °C, 5 h at 400 °C) | 98.8 | 0.047 | 0.039 |

[a]The BET surface area measured from $N_2$ adsorption isotherm using the BET method. [b]Mesopore volume measured from $N_2$ adsorption isotherm using the BJH method. [c]Micropore volume measured from $N_2$ adsorption isotherm using the *t*-plot method.

To summarize, the reaction temperature plays an important role in affecting the selectivity for the target product and the lifetime of the hybrid catalyst during the $CO_2$ hydrogenation reaction. Under high-temperature conditions, the formation rate of coke is slow; there are few hydrocarbon pool species, and the yield of olefins is low. Low temperatures can promote both the production of active hydrocarbon pool species and inactive light coke (adamantane species), resulting in acid sites being covered, pore channels being blocked, and finally, catalysts being deactivated. After regeneration at high temperatures, the harmful light coke is decomposed and transformed into polymethylbenzenes, so the active hydrocarbon pool species can be built up quickly after this transient temperature treatment, which consists of first low and subsequently high-temperature reactions, contributing to an increased selectivity for olefins. More details will be discussed in the following sections.

**3.3. Effect of Pressure on the Reactivity and Evolution of Coke.** The influence of various reaction pressures was investigated next at a reaction temperature of 325 °C over the hybrid catalysts of $In_2O_3$ and SSZ-13 (SSZ-13-25) zeolite. The detailed catalytic performances of these are presented in Figure S8. Table 2 and Figure 7a reveal the significant effect that reaction pressure has on the selectivity for olefins and the stability of catalysts. When the pressure increased from 10 to 40 bar, a negative effect of reaction pressure was found on the stability of the catalyst. At 10 bar, the catalyst had higher stability at 325 °C, and the selectivity for light olefins (based on HCs only) exceeded 80% after 12 h TOS without any deactivation. When the pressure was increased from 10 to 40 bar, the catalyst underwent serious deactivation, indicated by increases in the selectivity for methane and unreacted methanol in the effluent, which started after only 2.5 h at 40 bar. As discussed earlier, when using a fixed feed ratio of $H_2$ and $CO_2$, increasing the total pressure increases the partial pressure of both hydrogen and methanol simultaneously, as shown in Table 2. It has been shown that increasing the partial pressure of hydrogen cofeed can inhibit the deposition of coke significantly and improve the lifetime of the HSAPO-34 catalyst (the reaction lifetime extended from 3

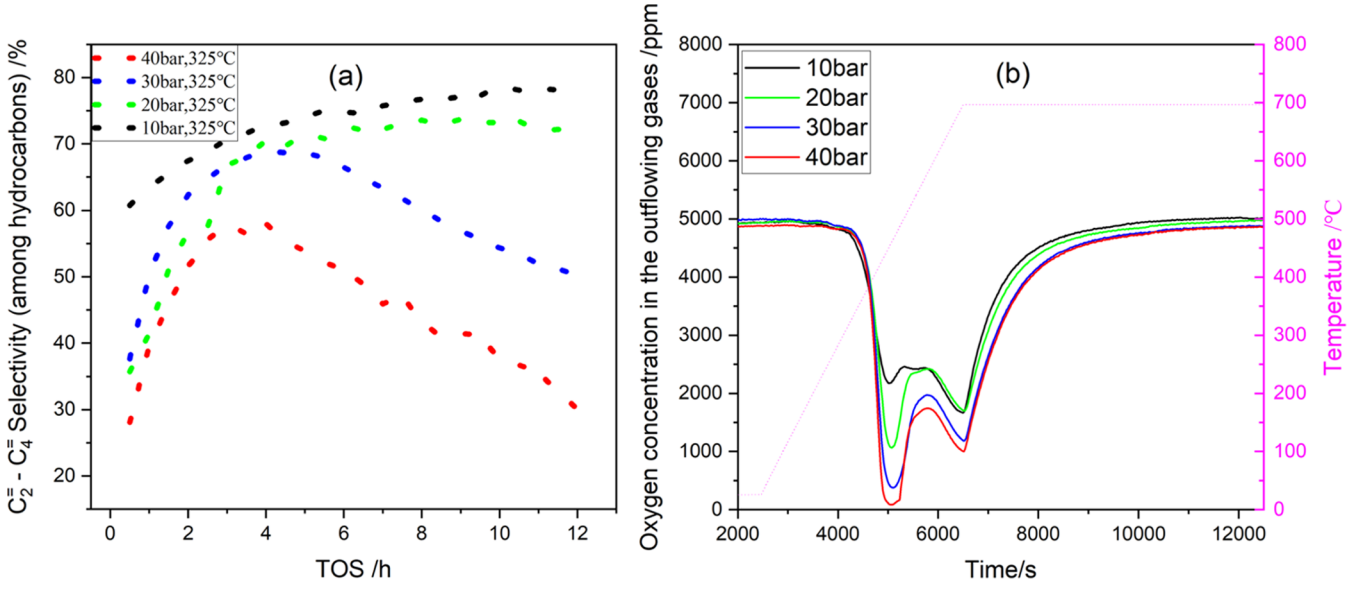


**Figure 7.** Alkene selectivity ($C_2^=$ to $C_4^=$) during $CO_2$ hydrogenation over the granule mixture $In_2O_3$/SSZ-13-25 under different pressures (a) and TPO profiles of the coke in the corresponding spent catalysts after 12 h of reaction (b). Reaction conditions: catalyst weight = 1 g, weight ratio of $In_2O_3$/SSZ-13-25 = 2 in granule mixture, GHSV = 6400 N mL/(g h), $T$ = 325 °C, $H_2/CO_2$ = 6, and TOS = 12 h.


https://doi.org/10.1021/acs.energyfuels.3c03172
Energy Fuels XXXX, XXX, XXX−XXX

**Scheme 1. Proposed Reaction Network of Coke Species for $CO_2$ Hydrogenation over the $In_2O_3$/SSZ-13 Catalyst**

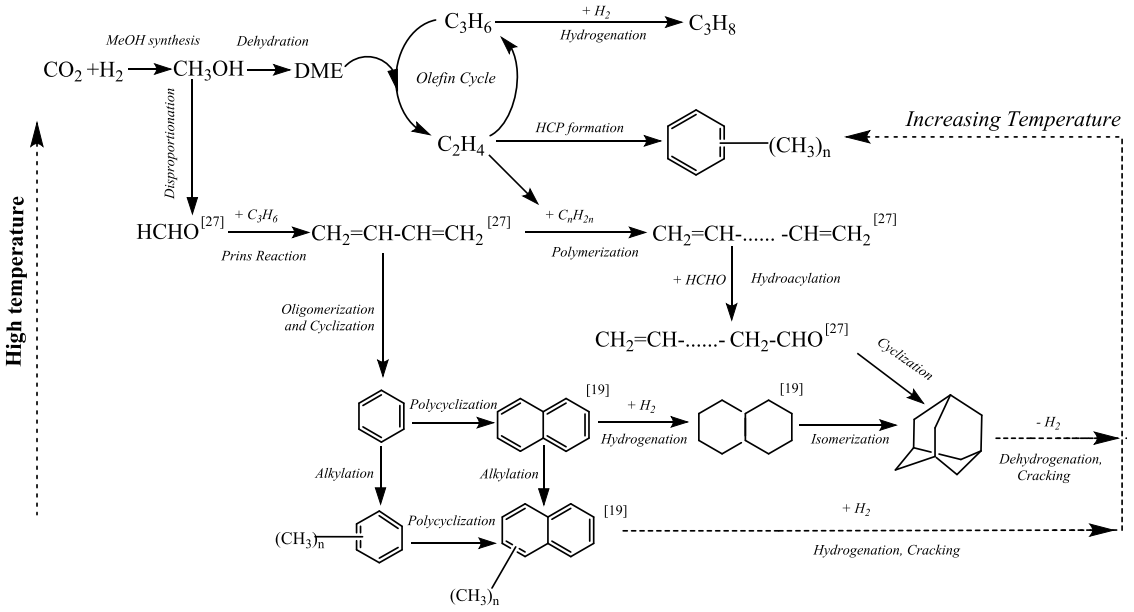


to 93 h when the partial pressure of hydrogen increased from 4.3 to 21.4 bar) in MTO process.[19] But it is apparent here that increasing the partial pressure of methanol can greatly weaken the effect of the hydrogen partial pressure to prolong the catalyst lifetime, as shown in similar results reported by Nieskens et al.[16] Hwang et al. demonstrated that the correlation between the increase in the formation of methane and increased methanol partial pressure reflects the improved rate of formation of formaldehyde from methanol disproportionation over HSSZ-13 zeolite. Moreover, formaldehyde participates further in alkylation of the hydrocarbon pool, leading to deactivation of the HSSZ-13 zeolite during the MTO reaction. More specifically, formaldehyde is involved in the Prins reaction, reacting with alkene to form dienes, active aromatics, and inactive polycyclic aromatic species.[27] Recent reports have also revealed that hydrogen prevents formaldehyde-mediated alkylation reactions during the coprocessing of $H_2$ with formaldehyde and methanol.[18,20,47] However, at low temperatures, the effect of the hydrogenation reaction is too weak to block the aggregation of coke promoted by formaldehyde; therefore, a faster deactivation and a more rapid coke formation occur under conditions of low temperature and high pressure.

Furthermore, during the reaction at 325 °C, a large amount of light coke was found in the deactivated catalyst after the reaction at high pressure (40 bar), but a lesser amount was present in the non-deactivated catalyst after the low-pressure reaction (10 bar), as can be seen in Figure 7b (details given in Figure S9). This result further confirms that the formation of light coke (adamantane species) was the main cause of catalyst deactivation at low temperatures; in particular, it reveals the important correlation between the reaction pressure and the formation of light coke. Previous studies have suggested that the formation of adamantane under a hydrogen atmosphere is related to the continued isomerization of hydrogenation products from unsaturated aromatics.[19] Whereas in the hydrogen-free atmosphere of the MTO reaction, its formation is attributed mainly to the cyclization of dienes to generate cycloalkanes and subsequent isomerization of cycloalkanes to adamantanes at low temperatures.[42] Based on the above two possible formation paths, there is inadequate evidence to determine which path plays an important role in the formation of adamantane during $CO_2$ hydrogenation, but there is nevertheless sufficient evidence to suspect that formaldehyde plays a key role in the formation of adamantane at a low temperature. The higher reaction pressure accelerates the formation of formaldehyde, which forms inactive adamantane by oligomerization and cyclization and eventually results in the final deactivation of the zeolite catalyst.

**3.4. Reaction Network for Coke Evolution.** An overall network of coke evolution can now be proposed, as illustrated in Scheme 1. When $CO_2$ hydrogenation is carried out at a high temperature (close to 400 °C), the amount of coke deposition inside the SSZ-13 zeolite is low, and the rates of hydrogenation and dehydration reactions over acid sites are fast. Following dehydration to generate DME, most of the input methanol is preferentially converted into propylene through the olefin cycle and then further hydrogenated to propane on acid sites. Specifically, due to the high concentration of water generated by the high conversion rate of $CO_2$ at high temperatures (main contribution from RWGS), under the synergistic effect of water and hydrogen, the formation of coke precursors (formaldehyde and dienes) is inhibited. Also, the cyclization of dienes to HCP species and coke is interrupted, and thus, the rate of coke accumulation slows down, resulting in a low deposition rate of coke as well as low selectivity for olefins. When the reaction is performed at a low temperature (close to 300 °C), the rates of dehydration reactions decrease. This results in an excess of methanol inside zeolite, which accelerates the disproportionation reaction of methanol, especially under the higher methanol partial pressure, resulting in a rapid increase in the formaldehyde product as the main coke precursor. Moreover, the hydrogenation reaction, which has an inhibitory effect on the formation of coke precursors, is weakened at a low temperature. The polymerization, hydroacylation,[27] and cyclization of the coke precursors (formaldehyde, diene, polyoxymethylene) is accelerated; thus, the rate of HCP and coke formation increases drastically. Especially the HCP acts as a self-catalyst to boost the conversion of methanol to olefins through the aromatic cycle.


https://doi.org/10.1021/acs.energyfuels.3c03172
Energy Fuels XXXX, XXX, XXX−XXX

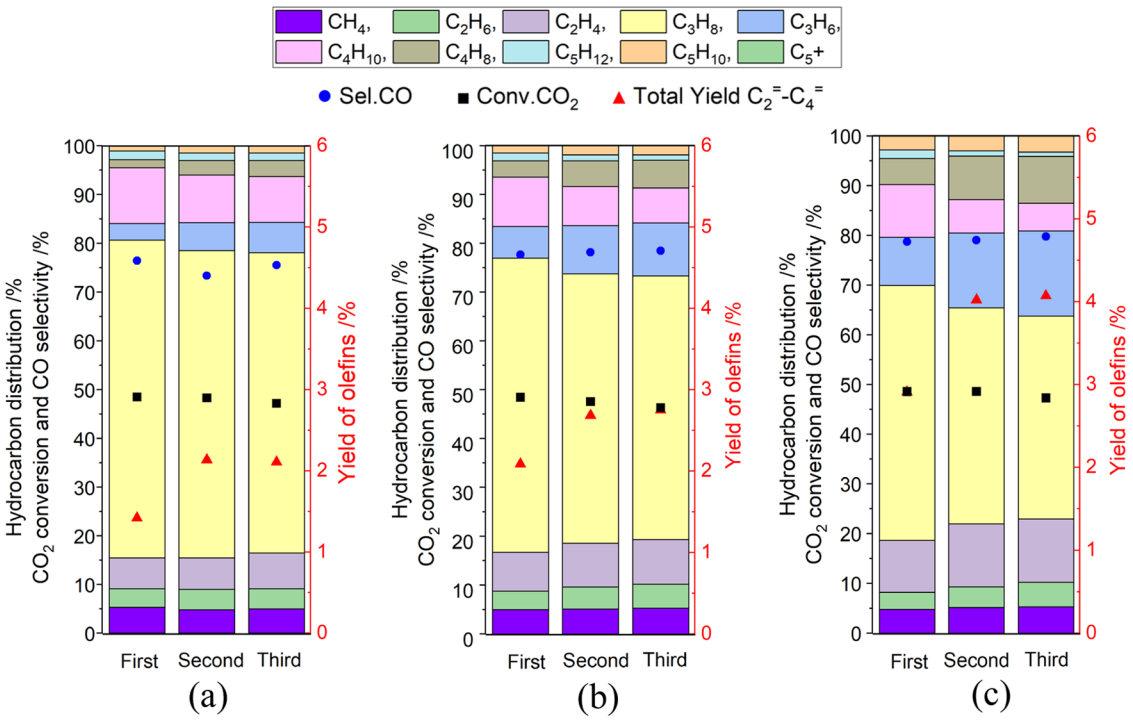


**Figure 8.** Catalytic performance of $In_2O_3$/SSZ-13-15 (a), $In_2O_3$/SSZ-13-20 (b), and $In_2O_3$/SSZ-13-25 (c) before and after coking treatments during the continuous transient experiment. In the transient experiment, the temperature variation sequence is as follows: 5 h at 400 °C → 20 h at 325 °C → 5 h at 400 °C → 10 h at 325 °C → 5 h at 400 °C. The notations "First", "Second", and "Third" refer to the reaction performance for fresh catalyst (TOS = 5 h), the performance after the first cycle of coking treatment (TOS = 30 h), and after the second cycle of coking treatment (TOS = 45 h), respectively. Reaction conditions: catalyst weight = 1 g, weight ratio of oxidate/zeolite = 2 in granule mixture, GHSV = 6400 N mL/(g h), $T$ = 400 °C, $P$ = 30 bar, and $H_2/CO_2$= 6.

At the same time, coke also covers part of the strong acid sites to inhibit further hydrogenation of the olefins, resulting in a temporarily high yield of olefins at low temperatures. However, the excessive build-up of coke precursors (such as formaldehyde) also promotes the formation of harmful light adamantane through oligomerization and cyclization reactions. This adamantane deposits inside the zeolite's porous structure, covering the active centers, hindering mass transfer, and, finally, leading to deactivation. Upon switching the process to a high temperature, these adamantanes can be converted rapidly into small active aromatics by cracking reactions under an atmosphere of hydrogen and water, leaving mostly HCP species in the catalyst. As the active coke species are partially preserved and harmful ones are decomposed, the catalyst activity is thus restored.

Under different partial pressures of hydrogen, water, and methanol, temperature plays an important role in controlling the formation and decomposition of coke. Hydrogenation and cracking reactions inhibit or interrupt the formation and proliferation of coke, while the disproportionation, aromatization, and cyclization reactions promote the deposition of coke. When these reactions reach a dynamic balance at an optimized temperature and specific partial pressure, the accumulation of active hydrocarbon pool species will also reach a dynamic equilibrium within the catalysts, and consequently, the catalyst lifetime will be prolonged.

**3.5. Role of Acid Density on the Modification of Coke.** Inspired by the rapid accumulation of hydrocarbon pool species that resulted from the high and low-temperature treatments, a continuous transient experiment (5 h at 400 °C → 20 h at 325 °C→ 5 h at 400 °C → 10 h at 325 °C → 5 h at 400 °C) was carried out to study the catalytic properties of the catalysts with various levels of acidity before and after the coke modification steps at 325 °C. The performances of $In_2O_3$/SSZ-13-15, $In_2O_3$/SSZ-13-20, and $In_2O_3$/SSZ-13-25 were recorded in detail during $CO_2$ hydrogenation, as shown in Figure S10 and Tables S3 and S4. Since the same $In_2O_3$ catalyst was used for methanol synthesis in all catalysts, the $CO_2$ conversion was almost independent of the differences in the zeolites and changed only with the reaction temperature. In the initial stage at 400 °C, and as the reaction progressed, coke accumulated gradually and the selectivity for light olefins increased steadily. When the reaction temperature was switched to 325 °C, all of the catalysts began to deactivate: the lower the acid density of the catalyst, the faster the rate of deactivation. The $In_2O_3$/SSZ-13-15 showed the longest lifetime of 5 h at 325 °C, followed by $In_2O_3$/SSZ-13-20 and $In_2O_3$/SSZ-13-25. When the reaction conditions returned to the second 400 °C stage, the activity and performance of all catalysts were well restored. A volcanic olefin yield curve was displayed again in the second stage of the reaction at 325 °C with deactivation indicated by methanol breakthrough in the effluent occurring more quickly. This indicated that the regeneration effect of high-temperature treatment was universally applicable, irrespective of the acid density of the catalyst.

The experimental results shown in Figure S10 (5 h at 400 °C → 20 h at 325 °C→ 5 h at 400 °C → 10 h at 325 °C → 5 h at 400 °C) are summarized in Figure 8, where the steady-state results at TOS of 5, 30, and 45 h are selected for comparison since they are under the same reaction conditions but following the different reaction periods, which are denoted as "first, second, and third" in Figure 8. The conversion of $CO_2$


https://doi.org/10.1021/acs.energyfuels.3c03172
Energy Fuels XXXX, XXX, XXX−XXX

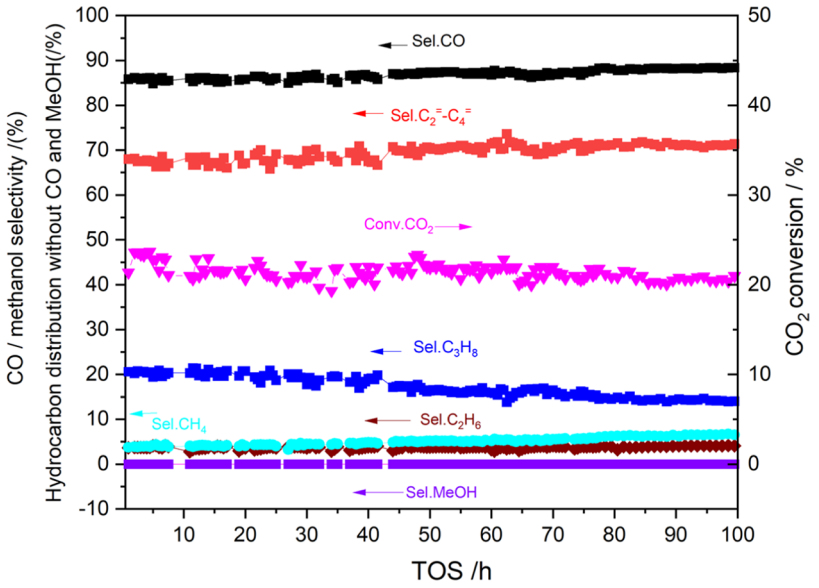


**Figure 9.** Long-term catalytic performance of precoked catalyst $In_2O_3$/SSZ-13-25 in $CO_2$ hydrogenation. Precoking procedure: 325 °C for 20 h and then 400 °C for 5 h under GHSV = 6400 N mL/(g h), $H_2/CO_2$= 6, $P$ = 30 bar. Reaction conditions: catalyst weight = 1 g, weight ratio of $In_2O_3$/SSZ-13-25 = 2 in granule mixture, GHSV = 6400 N mL/(g h), $P$ = 20 bar, $H_2/CO_2$ = 3, and $T$ = 375 °C.

and the selectivity for CO remained stable for each individual catalyst after the coking treatments at 325 °C, while the selectivity for olefins had improved greatly: more specifically, the yield of propylene increased more significantly than that of ethylene. Since it was only the accumulation of coke that altered the property of the zeolites, it did not affect the $In_2O_3$ that was responsible for the $CO_2$ conversion. The increased yields of ethylene and propylene after the coking treatments indicated that the accumulation of hydrocarbon pool species increased, and the stronger increase of selectivity of propylene also implies that the further hydrogenation of olefins was weakened too. However, the accumulation of hydrocarbon pool species also had a dynamic equilibrium after a sufficient duration of the coking treatment at certain reaction conditions. After a second round of the coking treatment, the selectivity for olefins did not increase further at 400 °C (comparison between the "Second" and "Third" stage performance in Figure 8), thereby indicating that a steady state had been established in the catalysts.

The results also indicate that when comparing catalysts of varying acid densities, the $In_2O_3$/SSZ-13-25 catalyst with a zeolite component containing the lowest acid density showed the highest selectivity for olefins after two coking treatments. The detailed characterization of coke taken from the modified catalysts after two rounds of coking treatments in the transient experiments is shown in Figures S11−S13. It is obvious that, as with the catalyst after the first round of coking treatment (20 h at 325 °C followed by 5 h at 400 °C, Figure 3b), most of the polymethylbenzene species were preserved as soluble coke species within the spent catalysts after the second round of treatment. The TPO results confirmed further that no inactive adamantanes were present inside the catalysts. The quantitative results of TPO profiles also disclosed that the catalyst with the lower acid density had a more rapid coke deposition rate, which concurs with the TGA results. As discussed previously, at 400 °C, active methylbenzene species are the main soluble species present in the deposited coke. With a faster rate of coke deposition, more hydrocarbon pool species accumulated and caused higher selectivity and yields of olefins (Figure S14). In contrast, at 325 °C, inactive polycyclic aromatic hydrocarbons and adamantane species both form in the catalyst, and thus, more of these inactive species are formed as the coke deposition rate increases. Therefore, a less acidic catalyst is deactivated rapidly in a shorter period at low temperatures, but it can exhibit a high olefin selectivity at a higher temperature when these inactive coke deposits are converted into hydrocarbon pool species. It is worth mentioning here that the acidity is not constant as the reaction progresses. As the deposition of coke accumulates, the acid density of the catalyst continues to decrease. This changes the diffusion properties of the channels, which, in turn, will affect the rate of coke deposition.

**3.6. Stability of Precoked Catalysts.** Thus, so far, it has been seen that coking can be used to successfully modify a hybrid catalyst containing a low acid density SSZ-13 zeolite component to achieve a high olefin selectivity (Figure 8c). Different optimizations of the conditions for precoking and reaction were conducted, which is discussed in the Supporting Information together with Figures S15 and S16. The best conditions found were precoking at 325 °C for 20 h and then 400 °C for 5 h using $H_2/CO_2$ = 6, $P$ = 30 bar, followed by an activity experiment at 375 °C. This resulted in a very stable activity with light olefin selectivity (based on formed HCs) up to 70%, CO selectivity of 88%, and $CO_2$ conversion of 20% with no obvious deactivation after 100 h on the stream, as shown in Figure 9. Compared with the result of the fresh catalyst under the same reaction conditions (Figure S17), the precoking treatment plays an important role in stabilizing the active sites and shortening the time to achieve stable production of light olefins. This is mostly due to the rapid deposition of hydrocarbon pool species and the adjustment of catalyst acidity by its deposition. So, a balance between coke deposition and decomposition is quickly established based on this adjusted acidity under suitable reaction conditions. More detailed characterization (Figures S18−S20) of the precoked catalyst before and after the reaction supported these findings. For the precoked catalyst before the 100 h reaction test, the main deposited coke species were methylbenzenes, and the


https://doi.org/10.1021/acs.energyfuels.3c03172
Energy Fuels XXXX, XXX, XXX−XXX

total amount of coke was 2.4 wt %. After running for 100 h, no adamantane species were generated, and only a larger quantity of methylbenzene species with small amounts of polycyclic aromatic coke were generated. Also, after 100 h of TOS, the total amount of deposited coke was 4.0 wt %, indicating an almost steady state for the formation and decomposition of coke during the whole reaction period. Finally, the complete removal of coke deposited on the catalyst may require the use of stripping or oxidative combustion techniques.[48] However, optimized reaction conditions, as well as an appropriate precoking treatment, can greatly increase the efficiency of the catalyst, so the development of fixed bed technology or moving bed technology for olefin production from $CO_2$ hydrogenation has become possible.

## 4. CONCLUSIONS

It has been discovered that the coking properties of the SSZ-13 zeolite in hybrid catalysts are affected significantly by temperature and pressure during the process of hydrogenating $CO_2$ into olefins, which affects the lifetime of the catalyst and the selectivity for olefins produced. In contrast to the pure MTO reaction process, the coexistence of hydrogen with more water, along with methanol resulting from the simultaneous methanol synthesis process, affects the overall performance of the SSZ-13 zeolite for MTO reactions. At a high temperature (around 400 °C), the hydrogenation and cracking reactions inhibit the accumulation of both coke and hydrocarbon pool species and prolong the lifetime of the SSZ-13 zeolite and also produce a large amount of alkanes due to the excessive hydrogenation of olefins on acid sites. At a low temperature (around 325 °C), on the other hand, the increased methanol disproportionation reactions accelerate the formation of coke and promote, especially, the formation of inactive adamantane species at low temperature (325 °C) and high pressure (40 bar). This results in the blockage of zeolite channels and the coverage of acid centers, thereby causing the rapid deactivation of the zeolite. However, these adamantane species can be decomposed rapidly into small aromatics at high temperatures (around 400 °C), which not only restores the activity of the SSZ-13 zeolite but also promotes the accumulation of hydrocarbon pool species and inhibits the strong acidic sites. After a transient temperature coking treatment with low temperature (325 °C) for accumulation and high temperature (400 °C) for regeneration, the active sites of the SSZ-13 zeolite can be modulated well to give a higher selectivity for olefins in the products, especially over SSZ-13 zeolite with a low acid density. Optimizing the reaction conditions further to match the acidity of the zeolite allows a steady state for the formation and decomposition of coke to be established, which is essential for the high stability of zeolites and the high selectivity for olefins during $CO_2$ hydrogenation. The stable performance of the precoked catalyst was finally verified by a long-term experiment, where the selectivity of light olefins was around 70% among hydrocarbons and no obvious deactivation was found during 100 h of operation.

## ASSOCIATED CONTENT

### Supporting Information

The Supporting Information is available free of charge at https://pubs.acs.org/doi/10.1021/acs.energyfuels.3c03172.

Detailed catalytic results and characterization results (PDF)

## AUTHOR INFORMATION


### Corresponding Author

**Derek Creaser** − *Chemical Engineering and Competence Centre for Catalysis, Chalmers University of Technology, Gothenburg 41296, Sweden;* orcid.org/0000-0002-5569-5706; Email: derek.creaser@chalmers.se

### Authors

**Wei Di** − *Chemical Engineering and Competence Centre for Catalysis, Chalmers University of Technology, Gothenburg 41296, Sweden*

**Abdenour Achour** − *Chemical Engineering and Competence Centre for Catalysis, Chalmers University of Technology, Gothenburg 41296, Sweden*

**Phuoc Hoang Ho** − *Chemical Engineering and Competence Centre for Catalysis, Chalmers University of Technology, Gothenburg 41296, Sweden*

**Sreetama Ghosh** − *Chemical Engineering and Competence Centre for Catalysis, Chalmers University of Technology, Gothenburg 41296, Sweden*

**Oleg Pajalic** − *Perstorp Specialty Chemicals AB, Perstorp 28480, Sweden*

**Lars Josefsson** − *Josefsson Sustainable Chemistry AB, Stenungsund 44448, Sweden*

**Louise Olsson** − *Chemical Engineering and Competence Centre for Catalysis, Chalmers University of Technology, Gothenburg 41296, Sweden;* orcid.org/0000-0002-8308-0784

Complete contact information is available at: https://pubs.acs.org/10.1021/acs.energyfuels.3c03172


### Notes

The authors declare no competing financial interest.

## ACKNOWLEDGMENTS

This work was conducted at the Chemical Engineering division, the Competence Center for Catalysis (KCK), and the Center for Process Chemical Engineering (CPE), Chalmers University of Technology, and was performed in collaboration with Perstorp AB and Josefsson Sustainable Chemistry AB. The authors gratefully acknowledge the funding from the Swedish Energy Agency (P49617-1). The authors also thank Dr. Andreas Schaefer for his help with XRF measurements.

## REFERENCES


(1) Aresta, M.; Dibenedetto, A.; Angelini, A. Catalysis for the Valorization of Exhaust Carbon: From $CO_2$ to Chemicals, Materials, and Fuels. Technological Use of $CO_2$. *Chem. Rev.* **2014**, *114*, 1709−1742.

(2) Yang, H.; Zhang, C.; Gao, P.; Wang, H.; Li, X.; Zhong, L.; Wei, W.; Sun, Y. A review of the catalytic hydrogenation of carbon dioxide into value-added hydrocarbons. *Catal. Sci. Technol.* **2017**, *7*, 4580−4598.

(3) Ronda-Lloret, M.; Rothenberg, G.; Shiju, N. R. A Critical Look at Direct Catalytic Hydrogenation of Carbon Dioxide to Olefins. *ChemSusChem* **2019**, *12*, 3896−3914.

(4) Ojelade, O. A.; Zaman, S. A review on $CO_2$ hydrogenation to lower olefins: Understanding the structure-property relationships in heterogeneous catalytic systems. *J. $CO_2$ Util.* **2021**, *47*, No. 101515.

(5) Frei, M. S.; Capdevila-Cortada, M.; García-Muelas, R.; Mondelli, C.; López, N.; Stewart, J. A.; Ferré, D.; Pérez-Ramírez, J. Mechanism and microkinetics of methanol synthesis via $CO_2$ hydrogenation on indium oxide. *J. Catal.* **2018**, *361*, 313−321.

(6) Ye, R.-P.; Ding, J.; Gong, W.; Argyle, M. D.; Zhong, Q.; Wang, Y.; Russell, C. K.; Xu, Z.; Russell, A. G.; Li, Q.; Fan, M.; Yao, Y. G. $CO_2$ Hydrogenation to High-Value Products via Heterogeneous Catalysis. *Nat. Commun.* **2019**, *10*, No. 5698.
(7) Witoon, T.; Lapkeatseree, V.; Numpilai, T.; Cheng, C. K.; Limtrakul, J. $CO_2$ hydrogenation to light olefins over mixed Fe-Co-K-Al oxides catalysts prepared via precipitation and reduction methods. *Chem. Eng. J.* **2022**, *428*, No. 131389.
(8) Li, Z.; Wang, J.; Qu, Y.; Liu, H.; Tang, C.; Miao, S.; Feng, Z.; An, H.; Li, C. Highly Selective Conversion of Carbon Dioxide to Lower Olefins. *ACS Catal.* **2017**, *7*, 8544−8548.
(9) Liu, X.; Wang, M.; Zhou, C.; Zhou, W.; Cheng, K.; Kang, J.; Zhang, Q.; Deng, W.; Wang, Y. Selective transformation of carbon dioxide into lower olefins with a bifunctional catalyst composed of $ZnGa_2O_4$ and SAPO-34. *Chem. Commun.* **2018**, *54*, 140−143.
(10) Gao, P.; Dang, S.; Li, S.; Bu, X.; Liu, Z.; Qiu, M.; Yang, C.; Wang, H.; Zhong, L.; Han, Y.; Liu, Q.; Wei, W.; Sun, Y. Direct Production of Lower Olefins from $CO_2$ Conversion via Bifunctional Catalysis. *ACS Catal.* **2018**, *8*, 571−578.
(11) Shi, Z.; Neurock, M.; Bhan, A. Methanol-to-Olefins Catalysis on HSSZ-13 and HSAPO-34 and Its Relationship to Acid Strength. *ACS Catal.* **2021**, *11*, 1222−1232.
(12) Tian, P.; Wei, Y.; Ye, M.; Liu, Z. Methanol to Olefins (MTO): From Fundamentals to Commercialization. *ACS Catal.* **2015**, *5*, 1922−1938.
(13) Yang, M.; Fan, D.; Wei, Y.; Tian, P.; Liu, Z. Recent Progress in Methanol-to-Olefins (MTO) Catalysts. *Adv. Mater.* **2019**, *31*, No. 1902181.
(14) Bailleul, S.; Yarulina, I.; Hoffman, A. E. J.; Dokania, A.; Abou-Hamad, E.; Chowdhury, A. D.; Pieters, G.; Hajek, J.; De Wispelaere, K.; Waroquier, M. J.; Gascon, J.; Van Speybroeck, V. A Supramolecular View on the Cooperative Role of Brønsted and Lewis Acid Sites in Zeolites for Methanol Conversion. *J. Am. Chem. Soc.* **2019**, *141*, 14823−14842.
(15) Zhou, J.; Gao, M.; Zhang, J.; Liu, W.; Zhang, T.; Li, H.; Xu, Z.; Ye, M.; Liu, Z. Directed transforming of coke to active intermediates in methanol-to-olefins catalyst to boost light olefins selectivity. *Nat. Commun.* **2021**, *12*, No. 17.
(16) Nieskens, D. L. S.; Lunn, J. D.; Malek, A. Understanding the Enhanced Lifetime of SAPO-34 in a Direct Syngas-to-Hydrocarbons Process. *ACS Catal.* **2019**, *9*, 691−700.
(17) Cheng, K.; Gu, B.; Liu, X.; Kang, J.; Zhang, Q.; Wang, Y. Direct and Highly Selective Conversion of Synthesis Gas into Lower Olefins: Design of a Bifunctional Catalyst Combining Methanol Synthesis and Carbon−Carbon Coupling. *Angew. Chem., Int. Ed.* **2016**, *55*, 4725−4728.
(18) Arora, S. S.; Nieskens, D. L. S.; Malek, A.; Bhan, A. Lifetime improvement in methanol-to-olefins catalysis over chabazite materials by high-pressure $H_2$ co-feeds. *Nat. Catal.* **2018**, *1*, 666−672.
(19) Zhao, X.; Li, J.; Tian, P.; Wang, L.; Li, X.; Lin, S.; Guo, X.; Liu, Z. Achieving a Superlong Lifetime in the Zeolite-Catalyzed MTO Reaction under High Pressure: Synergistic Effect of Hydrogen and Water. *ACS Catal.* **2019**, *9*, 3017−3025.
(20) DeLuca, M.; Janes, C.; Hibbitts, D. Contrasting Arene, Alkene, Diene, and Formaldehyde Hydrogenation in H-ZSM-5, H-SSZ-13, and H-SAPO-34 Frameworks during MTO. *ACS Catal.* **2020**, *10*, 4593−4607.
(21) Liu, Z.; Ni, Y.; Sun, T.; Zhu, W.; Liu, Z. Conversion of $CO_2$ and $H_2$ into propane over InZrOx and SSZ-13 composite catalyst. *J. Energy Chem.* **2021**, *54*, 111−117.
(22) Lu, S.; Yang, H.; Yang, C.; Gao, P.; Sun, Y. Highly selective synthesis of LPG from $CO_2$ hydrogenation over $In_2O_3$/SSZ-13 bifunctional catalyst. *J. Fuel Chem. Technol.* **2021**, *49*, 1132−1139.
(23) Olsbye, U.; Svelle, S.; Bjørgen, M.; Beato, P.; Janssens, T. V. W.; Joensen, F.; Bordiga, S.; Lillerud, K. P. Conversion of Methanol to Hydrocarbons: How Zeolite Cavity and Pore Size Controls Product Selectivity. *Angew. Chem., Int. Ed.* **2012**, *51*, 5810−5831.
(24) Chen, D.; Moljord, K.; Holmen, A. A methanol to olefins review: Diffusion, coke formation and deactivation on SAPO type catalysts. *Microporous Mesoporous Mater.* **2012**, *164*, 239−250.
(25) Zhou, J.; Zhi, Y.; Zhang, J.; Liu, Z.; Zhang, T.; He, Y.; Zheng, A.; Ye, M.; Wei, Y.; Liu, Z. Presituated "coke"-determined mechanistic route for ethene formation in the methanol-to-olefins process on SAPO-34 catalyst. *J. Catal.* **2019**, *377*, 153−162.
(26) Numpilai, T.; Wattanakit, C.; Chareonpanich, M.; Limtrakul, J.; Witoon, T. Optimization of synthesis condition for $CO_2$ hydrogenation to light olefins over $In_2O_3$ admixed with SAPO-34. *Energy Convers. Manage.* **2019**, *180*, 511−523.
(27) Hwang, A.; Kumar, M.; Rimer, J.; Bhan, A. Implications of methanol disproportionation on catalyst lifetime for methanol-to-olefins conversion by HSSZ-13. *J. Catal.* **2017**, *346*, 154−160.
(28) Frei, M. S.; Mondelli, C.; García-Muelas, R.; et al. Atomic-scale engineering of indium oxide promotion by palladium for methanol production via $CO_2$ hydrogenation. *Nat. Commun.* **2019**, *10*, No. 3377.
(29) Araújo, T. P.; Shah, A.; Mondelli, C.; Stewart, J. A.; Ferré, D. C.; Pérez-Ramírez, J. Impact of hybrid $CO_2$-CO feeds on methanol synthesis over $In_2O_3$-based catalysts. *Appl. Catal., B* **2021**, *285*, No. 119878.
(30) Di Iorio, J. R.; Gounder, R. Controlling the isolation and pairing of aluminum in chabazite zeolites using mixtures of organic and inorganic structure-directing agents. *Chem. Mater.* **2016**, *28*, 2236−2247.
(31) Wang, Y.; Wang, G.; van der Wal, L. I.; Cheng, K.; Zhang, Q.; de Jong, K. P.; Wang, Y. Visualizing Element Migration over Bifunctional Metal-Zeolite Catalysts and its Impact on Catalysis. *Angew. Chem.* **2021**, *133*, 17876−17884.
(32) Bhawe, Y.; Moliner-Marin, M.; Lunn, J. D.; Liu, Y.; Malek, A.; Davis, M. Effect of Cage Size on the Selective Conversion of Methanol to Light Olefins. *ACS Catal.* **2012**, *2*, 2490−2495.
(33) Di, W.; Ho, P. H.; Achour, A.; Pajalic, O.; Josefsson, L.; Olsson, L.; Creaser, D. $CO_2$ hydrogenation to light olefins using $In_2O_3$ and SSZ-13 catalyst− Understanding the role of zeolite acidity in olefin production. *J. $CO_2$ Util.* **2023**, *72*, No. 102512.
(34) Usui, T.; Liu, Z.; Ibe, S.; Zhu, J.; Anand, C.; Igarashi, H.; Onaya, N.; Sasaki, Y.; Shiramata, Y.; Kusamoto, T.; Wakihara, T. Improve the hydrothermal stability of Cu-SSZ-13 zeolite catalyst by loading a small amount of Ce. *ACS Catal.* **2018**, *8*, 9165−9173.
(35) Kumar, M.; Luo, H.; Román-Leshkov, Y.; Rimer, J. D. SSZ-13 Crystallization by Particle Attachment and Deterministic Pathways to Crystal Size Control. *J. Am. Chem. Soc.* **2015**, *137*, 13007−13017.
(36) Hwang, A.; Bhan, A. Bifunctional Strategy Coupling $Y_2O_3$-Catalyzed Alkanal Decomposition with Methanol-to-Olefins Catalysis for Enhanced Lifetime. *ACS Catal.* **2017**, *7*, 4417−4422.
(37) Ghosh, S.; Sebastian, J.; Olsson, L.; Creaser, D. Experimental and kinetic modeling studies of methanol synthesis from $CO_2$ hydrogenation using $In_2O_3$ catalyst. *Chem. Eng. J.* **2021**, *416*, No. 129120.
(38) Xie, J.; Firth, D. S.; Cordero-Lanzac, T.; Airi, A.; Negri, A.; Øien-degaard, S.; Lillerud, K. P.; Bordiga, S.; Olsbye, U. MAPO-18 Catalysts for the Methanol to Olefins Process: Influence of Catalyst Acidity in a High-Pressure Syngas (CO and $H_2$) Environment. *ACS Catal.* **2022**, *12*, 1520−1531.
(39) Wang, H.; Hou, Y.; Sun, W.; Hu, Q.; Xiong, H.; Wang, T.; Yan, B.; Qian, W. Insight into the Effects of Water on the Ethene to Aromatics Reaction with HZSM-5. *ACS Catal.* **2020**, *10*, 5288−5298.
(40) Borodina, E.; Meirer, F.; Lezcano-González, I.; Mokhtar, M.; Asiri, A. M.; Al-Thabaiti, S. A.; Basahel, S. N.; Ruiz-Martinez, J.; Weckhuysen, B. M. Influence of the Reaction Temperature on the Nature of the Active and Deactivating Species during Methanol to Olefins Conversion over H-SSZ-13. *ACS Catal.* **2015**, *5*, 992−1003.
(41) Ghosh, S.; Olsson, L.; Creaser, D. Methanol mediated direct $CO_2$ hydrogenation to hydrocarbons: Experimental and kinetic modeling study. *Chem. Eng. J.* **2022**, *435*, No. 135090.
(42) Wei, Y.; Li, J.; Yuan, C.; Xu, S.; Zhou, Y.; Chen, J.; Wang, Q.; Zhang, Q.; Liu, Z. Generation of diamondoid hydrocarbons as


https://doi.org/10.1021/acs.energyfuels.3c03172
Energy Fuels XXXX, XXX, XXX−XXX

confined compounds in SAPO-34 catalyst in the conversion of methanol. *Chem. Commun.* **2012**, *48*, 3082−3084.
(43) Bjorgen, M.; Svelle, S.; Joensen, F.; Nerlov, F.; Kolboe, F.; Bonino, F.; Palumbo, L.; Silvia Bordiga, S.; Olsbye, U. Conversion of methanol to hydrocarbons over zeolite H-ZSM-5: On the origin of the olefinic species. *J. Catal.* **2007**, *249*, 195−207.
(44) Bordiga, S.; Regli, L.; Cocina, D.; Lamberti, C.; Bjørgen, M.; Lillerud, K. P. Assessing the Acidity of High Silica Chabazite H - SSZ-13 by FTIR Using CO as Molecular Probe: Comparison with H-SAPO-34. *J. Phys. Chem. B* **2005**, *109*, 2779−2784.
(45) Ravi, M.; Sushkevich, V. L.; van Bokhoven, J. A. On the location of Lewis acidic aluminum in zeolite mordenite and the role of framework-associated aluminum in mediating the switch between Brønsted and Lewis acidity. *Chem. Sci.* **2021**, *12*, 4094−4103.
(46) Skarlis, S. A.; Berthout, D.; Nicolle, A.; Dujardin, C.; Granger, P. IR Spectroscopy Analysis and Kinetic Modeling Study for $NH_3$ Adsorption and Desorption on H- and Fe-BEA Catalysts. *J. Phys. Chem. C* **2013**, *117*, 7154−7169.
(47) Liu, Y.; Kirchberger, F. M.; Müller, S.; et al. Critical role of formaldehyde during methanol conversion to hydrocarbons. *Nat. Commun.* **2019**, *10*, No. 1462.
(48) Portillo, A.; Ateka, A.; Ereña, J.; Bilbao, J.; Aguayo, A. T. Alternative acid catalysts for the stable and selective direct conversion of $CO_2$/CO mixtures into light olefins. *Fuel Process. Technol.* **2022**, *238*, No. 107513.


https://doi.org/10.1021/acs.energyfuels.3c03172
*Energy Fuels* XXXX, XXX, XXX−XXX